https://doi.org/10.5194/egusphere-2022-198
Preprint. Discussion started: 6 May 2022

DSCIM-Coastal v1.0: An Open-Source Modeling Platform for Global Impacts of Sea Level Rise

Nicholas Depsky[1,3,*], Ian Bolliger[2,3,*,†], Daniel Allen[3], Jun Ho Choi[6], Michael Delgado[2], Michael Greenstone[4,6], Ali Hamidi[2], Trevor Houser[2], Robert E. Kopp[5], and Solomon Hsiang[3,4]

[1]Energy & Resources Group, University of California, Berkeley
[2]The Rhodium Group
[3]Global Policy Lab, Goldman School of Public Policy, University of California, Berkeley
[4]National Bureau of Economic Research
[5]Department of Earth & Planetary Sciences and Rutgers Institute of Earth, Ocean and Atmospheric Sciences, Rutgers University, New Brunswick, New Jersey, USA
[6]Energy Policy Institute, University of Chicago
[*]These authors contributed equally to this work.
[†]While this work was completed under the above affiliation, this author is now affiliated with BlackRock, San Francisco, California, USA.

Correspondence: Nicholas Depsky (njdepsky@berkeley.edu), Ian Bolliger (ian.bolliger@blackrock.com)

Abstract.

Global sea level rise (SLR) may impose substantial economic costs to coastal communities worldwide, but characterizing its global impact remains challenging because SLR costs depend heavily on natural characteristics and human investments at each location—including topography, the spatial distribution of assets, and local adaptation decisions. To date, several impact models have been developed to estimate global costs of SLR, yet the limited availability of open-source and modular platforms that easily ingest up-to-date socioeconomic and physical data sources limits the ability of existing systems to transparently incorporate new insights. In this paper, we present a modular open-source platform designed to address this need, providing end-to-end transparency from global input data to a scalable least-cost optimization framework that estimates adaptation and net SLR costs for nearly 10,000 global coastline segments and administrative regions. Our approach accounts both for uncertainty in the magnitude of global SLR and spatial variability in local relative sea level rise. Using this platform, we evaluate costs across 110 possible socioeconomic and SLR trajectories in the 21st century. We find annual global SLR costs of $180 billion to $200 billion in 2100 assuming optimal adaptation, moderate emissions (RCP 4.5) and middle-of-the-road (SSP 2) socioeconomic trajectories. Under the highest SLR scenarios modeled, this value ranges from $400 billion to $520 billion. We make this platform publicly available in an effort to spur research collaboration and support decision-making, with segment-level physical and socioeconomic input characteristics provided at https://doi.org/10.5281/zenodo.6449231, source code for this dataset at https://doi.org/10.5281/zenodo.6456115, the modeling framework at https://doi.org/10.5281/zenodo.6453099, and model results at https://doi.org/10.5281/zenodo.6014086.

https://doi.org/10.5194/egusphere-2022-198
Preprint. Discussion started: 6 May 2022

1 Introduction

Global mean sea level (GMSL) is projected to increase between 0.40-0.69 m for 2°C of warming and 0.58-0.91 m for 4°C of warming by 2100, though accelerated ice-sheet instability could result in substantially higher values (approaching 2 m) by end-of-century (Fox-Kemper et al., 2021). Coastal communities and ecosystems will experience a variety of impacts, including more frequent tidal flooding, higher extreme sea levels (ESLs)[1], erosion, wetland degradation, salinization of soils and water reservoirs, and loss of land area to permanent inundation (Oppenheimer et al., 2019; Nicholls et al., 2006). The magnitude of relative sea level rise (RSLR) and associated impacts will vary by locality, depending upon global greenhouse gas (GHG) emissions (Fox-Kemper et al., 2021), ice sheet instabilities (DeConto et al., 2021; Bamber et al., 2019; Fox-Kemper et al., 2021), local atmosphere-ocean dynamics (Fox-Kemper et al., 2021), economic growth along coastlines (O'Neill et al., 2017; Neumann et al., 2015; Armstrong et al., 2016), and adaptation actions (Hinkel et al., 2018; Diaz, 2016; Hinkel et al., 2014; Lincke and Hinkel, 2021).

Despite advances in our understanding of GMSL, the global costs of these changes remain poorly constrained. A key obstacle to quantifying these global impacts is their strong dependence on the details of local conditions, such as topography, the spatial distribution of populations and assets, and local adaptation decisions. A challenge for modelers is the dual objectives of fully accounting for these various factors at the local granularity necessary for accurate representation while also scaling these calculations globally. Improvements in computation and data availability now make achieving these two objectives feasible, but it has remained challenging for existing custom-built systems to be regularly updated to reflect new insights or improvements to global data sets describing local conditions.

This paper presents what is to our knowledge the first fully open-source coastal modeling platform that (i) integrates up-to-date local data on socioeconomic and physical conditions along coastlines globally, (ii) projects the physical, socioeconomic and ecological impacts of SLR along coastlines and (iii) directly models the costs and benefits of both retreat and protection as potential adaptation strategies. The platform is fulled coded in the open-source computer language Python (v3.9) and integrates recently released, satellite-augmented global data layers describing coastal elevations, local sea levels, and the distribution of population and physical capital with widely used socioeconomic datasets. These data layers are projected onto 9,087 unique coastal segments that span global coastlines. Each of these segments is then modeled as independently choosing across local, forward-looking adaptation strategies in an effort to minimize overall losses, following the framework developed in Diaz (2016). Using this platform, we evaluated net costs across 110 possible socioeconomic and SLR trajectories in the 21st century to present here, though the tool is capable of accommodating tens to hundreds of thousands of future simulations in parallel if desired.

We find annual global SLR costs of $180 billion to $200 billion in 2100 assuming optimal adaptation, moderate emissions (RCP 4.5) and middle-of-the-road (SSP 2) socioeconomic trajectories. Under the highest SLR scenarios modeled, this value ranges from $400 billion to $520 billion.

[1]Terminology and acronyms for concepts related to sea level align with those recommended for contemporary use in Gregory et al. (2019).

https://doi.org/10.5194/egusphere-2022-198
Preprint. Discussion started: 6 May 2022

All code used to aggregate and combine input data, as well as to estimate SLR impacts is publicly available. This encourages further development by the coastal impacts research community and modularizes the modeling process to facilitate seamless incorporation of future improvements to input datasets and additional model components.

1.1 The Basic Architecture of Global Coastal Impact Models

Global coastal models that estimate impacts of SLR and ESLs seek to quantify the exposure of some variable(s) of concern, such as human population, capital assets, and coastal ecosystems, to these physical hazards. They generally report the magnitude of exposure to these hazards as their final output, and convert this exposure into some outcome of interest, such as economic losses (Hinkel et al., 2014; Diaz, 2016; Lincke and Hinkel, 2018). These models usually contain spatially explicit representations of physical coastline characteristics (e.g. coast lengths, elevation and land surface areas), exposure variables, and physical hazard variables.

To estimate future impacts, global coastal models must assume or model trajectories of pertinent physical and socioeconomic values over time. Most climate change-oriented impacts models assess multiple trajectories of GMSL and many account for local RSLR and associated ESLs, which commonly correspond to different GHG emissions pathways (Hinkel et al., 2014; Diaz, 2016; Lincke and Hinkel, 2018, 2021). They may also contain different future trajectories of human population and capital asset growth, such as those represented in the Shared Socioeconomic Pathways (SSPs) database (Riahi et al., 2017; Hinkel et al., 2014; Lincke and Hinkel, 2018; Tiggeloven et al., 2020; Lincke and Hinkel, 2021).

The spatial and temporal resolution of model components can vary between studies and is sometimes limited by the resolution of available input datasets and/or by available computing resources. Additionally, many models also include some form of adaptive decision-making, such as allowing different coastal segments to construct protective coastal barriers (Hinkel et al., 2014; Diaz, 2016; Lincke and Hinkel, 2018; Tiggeloven et al., 2020; Lincke and Hinkel, 2021) or retreating inland (Diaz, 2016; Lincke and Hinkel, 2021), usually guided by some form of local cost-benefit analysis.

1.2 Closely Related Efforts and Platform Genealogy

Several past studies employed high-resolution global coastal impact models to estimate future damages from SLR and ESLs under various trajectories of global GHG emissions, socioeconomic scenarios, and adaptation pathways (Hinkel et al., 2014; Diaz, 2016; Lincke and Hinkel, 2018, 2021). Many of these studies used the Dynamic Interactive Vulnerability Assessment (DIVA) Coastal Database and modeling tool as their source of information for describing local coastlines. Originally developed by the Dynamic and Interactive Assessment of National, Regional and Global Vulnerability of Coastal Zones to Climate Change and Sea-Level Rise (DINAS-COAST) project (Vafeidis et al., 2008; Hinkel and Klein, 2009), the DIVA database partitions global coastlines into 12,148 segments and provides local physical attributes (e.g., inundation areas by elevation, extreme sea level heights, wetland areas, erosion characteristics) as well as socioeconomic characteristics (e.g. population densities, land use), allowing for more spatially disaggregated coastal impact analyses (Vafeidis et al., 2008; Hinkel and Klein, 2009). At the time of its initial release in 2008, DIVA represented a substantial improvement over previous global, coastal databases and impact studies, which were most commonly performed using data at much coarser spatial resolutions (Hoozemans et al., 1993;

https://doi.org/10.5194/egusphere-2022-198
Preprint. Discussion started: 6 May 2022

Yohe and Tol, 2002; Nicholls, 2004, 2002; Dronkers et al., 1990; Pardaens et al., 2011; Hinkel et al., 2013). Presently, however, the DINAS-COAST program is no longer funded, and the accessibility of the DIVA database has fluctuated. Recently, a landing page has been created for the DIVA model at http://diva.globalclimateforum.org, though as of early 2022 the corresponding dataset is only available via direct correspondence with its authors. The underlying code and input data used to construct the DIVA database is not publicly available, making it difficult to replicate prior studies' results and diagnose issues that have appeared in previous versions of the dataset (Sect. 2.5.1). In this work, we address these issues of accessibility and transparency by generating a publically-available global dataset of coastal socioeconomic metrics, updating all core data layers used to generate DIVA and releasing the data assimilation model used to aggregate these into the final data product. The full set of data updates are described in Sect. 2 below.

In a key early analysis, Hinkel et al. (2014) employed the DIVA database to model the combination of coastal flood damages and adaptation (specifically, protective levee construction) under twelve scenarios of future RSLR and socioeconomic projections for sub-national coastal zones. Sea level rise scenarios in this study were constructed from estimates of global thermal expansion and regional ocean dynamic sea level data corresponding to low-, medium-, and high-emissions Coupled Model Intercomparison Project Phase 5 (CMIP5) experiments (Taylor et al., 2012) (Representative Concentration Pathways 2.6, 4.5, and 8.5) in four Earth System Models (ESMs), combined with low, medium, and high land-ice scenarios. The study also evaluated two different digital elevation models (DEMs) for estimating population exposure in coastal floodplains to SLR and ESLs, the GLOBE DEM (GLO, 1999), which was the original DEM used in DIVA (Hinkel and Klein, 2009), and the more recent Shuttle Radar Topography Mission (SRTM) DEM (Rodriguez et al., 2005). They found that their results were highly sensitive to the choice of DEM, which underscores the importance of updating global data layers used in coastal impact modeling as improved products are made available, which is one of the central aims of the work we present in this paper.

Expanding on the approach of Hinkel et al. (2014), Diaz (2016) developed the Coastal Impact and Adaptation Model (CIAM), a global modeling tool that estimated 21st century costs and adaptation strategies for each DIVA segment. One core innovation presented in CIAM was that it allowed for each segment to choose between dike construction, as in Hinkel et al. (2014), and managed or reactive retreat. However, an obstacle to widespread usage of CIAM was its development in the commercial General Algebraic Modeling System (GAMS) closed-source platform. We build on the work by Diaz (2016), using the underlying decision-making framework of CIAM; however, we adapt, re-code, and optimize CIAM in the open-source Python computing language.

The architecture of CIAM was designed to capture key aspects of local adaptive decision-making that will likely be used by coastal communities worldwide. The objective of CIAM was to develop an optimization framework that could be applied locally, but generalized globally. To limit the computational challenge of solving stochastic dynamic programs for thousands of independent coastline segments, Diaz (2016) simplified the set of possible adaptation choices to a set of discrete decisions that are calibrated to local conditions. CIAM differentiated between six types of costs (a.k.a. "impacts" or "damages") due to RSLR and ESLs (Sect. 2.2): (a) the cost of permanent inundation of immobile capital or land, and ESL-related (b) damages to capital, (c) mortality, (d) expenditures on protection (i.e. infrastructure construction), (e) relocation costs, and (f) wetland loss. Possible protection actions include constructing levees at the 10, 100, 1000, and 10000-year ESL heights at each segment, and

https://doi.org/10.5194/egusphere-2022-198
Preprint. Discussion started: 6 May 2022

possible retreat actions include proactively vacating all land area under local mean sea level (MSL) or within the 10, 100, 1000, or 10000-year ESL floodplain. Simulations in CIAM are implemented using discreet time-steps, termed "adaptation planning periods" (40-50 years), during which each segment updates their retreat or protection height based on the maximum RSLR projected to occur within the period. CIAM also allows for modelers to select a "no planned adaptation" option that constrains retreat to to be reactive, rather than forward-looking, such that the population and capital assets only choose to relocate inland once they are permanently inundated by rising sea levels. Diaz (2016) considered a single socioeconomic growth trajectory based on the 2012 United Nations World Population Prospects (UN DESA, 2012), Penn World Table version 7.0 (Heston et al., 2011) and the 2011 IMF World Economic Outlook (IMF, 2011) projections and uses DIVA's older GLOBE DEM. The SLR trajectories used by Diaz (2016) were the 5th, 50th, and 95th percentiles of probabilistic RSLR projections from Kopp et al. (2014) for RCPs 2.6, 4.5, and 8.5, as well as a no-SLR baseline.

Here, we build on the approach of Diaz (2016), adapting and optimizing the decision-framework of CIAM to an entirely new set of global data inputs (i.e. replacing DIVA) and an open-source computer language. Given continued advancement in sea level rise modeling efforts and the improvement of global data inputs (e.g. coastal DEMs), it is essential that coastal impacts modeling platforms are able to integrate these updates. Additionally, we believe that these platforms should be developed in an open-source, transparent, and reproducible framework will allow for increased collaboration and more rapid iteration amongst coastal impacts researchers, as has done for modeling communities across numerous scientific disciplines (von Krogh and von Hippel, 2006). The platform we develop addresses these objectives by integrating the latest available physical, climate, and socioeconomic input data for an expanded suite of future SLR and economic growth trajectories in an updated and open-source version of the CIAM framework that, in addition to improved accessibility and transparency, results in greater resolution and substantially improved computational efficiency.

1.3 This Study: The Data-driven Spatial Climate Impact Model Coastal Impacts Architecture

This modeling platform was developed as the sea level rise impacts module of the Data-driven Spatial Climate Impact Model (**DSCIM**) architecture (Rode et al., 2021), and is thus named **DSCIM-Coastal**. It is partitioned into two distinct components, each made available as open-source products: (i) the collection of updated physical and socioeconomic input datasets by coastal segment, which is named the Sea Level Impacts Input Dataset by Elevation, Region, and Scenario, or **SLIIDERS**, and (ii) the modeling platform itself, called **pyCIAM** (short for "Python-based CIAM"). Both components have been developed in accordance with FAIR Guiding Principles for scientific data management (Wilkinson et al., 2016) that are intended to improve the Findability, Accessibility, Interoperability, and Reuse of scientific data.

The SLIIDERS data set is conceptually similar to DIVA in that it contains a suite of variables across a collection of coastal segments designed for coastal impact modeling efforts. However, while DIVA is not publicly accessible, SLIIDERS and all of its components are available with open access licenses, thereby supporting transparency and replicability of coastal damage analyses for research communities around the globe. In addition, the partition of global coastlines that defines separate coastal segments as units of analysis has been revamped in order to achieve greater balance in geographic coverage and reduce redundant computations.

https://doi.org/10.5194/egusphere-2022-198
Preprint. Discussion started: 6 May 2022

SLIIDERS is broken into two major elements, **SLIIDERS-ECON** and **SLIIDERS-SLR**. SLIIDERS-ECON contains updated topographic, geographic, and socioeconomic input datasets, including refined coastal DEMs, SLR projections, and socioeconomic growth trajectories. In SLIIDERS-SLR, we pair each coastal segment with the nearest projection of probabilistic RSLR from the LocalizeSL framework (Kopp et al., 2014, 2017) for 11 combinations of emissions scenario and ice sheet dynamics, resulting in a companion oceanographic dataset.

pyCIAM is an open-source, computationally efficient and functional modeling platform for segment-level adaptation decision making that incorporates the following improvements to the original implementation of CIAM (Diaz, 2016): (i) updates to (and expansion of) all input data (topographic, geographic, socioeconomic, and oceanographic) using SLIIDERS, (ii) improvements to model representation of different variables, such as population and capital asset distribution and storm damage calculations, (iii) availability as an open-source, self-contained Python package and input database, making the workflow easily accessible and modifiable for other researchers, and (iv) improved computational efficiency and scalability, enabling the application of CIAM to large, probabilistic ensembles of sea-level change.

The pyCIAM model is configured to utilize the SLIIDERS input data, but can easily be run using a modified set of inputs, provided the data structure matches that of SLIIDERS. Similarly, the SLIIDERS product can be used independently from pyCIAM as inputs for other coastal analysis or as contextual information on coastal zones. SLIIDERS consists of the model-ready inputs used in pyCIAM, as well as a collection of Python notebooks used for their construction from parent, raw data products. The pyCIAM package contains the model code itself, as well as a number of diagnostic and results visualization functions.

The following sections describe how SLIIDERS and pyCIAM were constructed, show example results of model outputs and diagnostics from 2000-2100 and compare to the results of Diaz (2016), and discuss current limitations to the model and input datasets, outlining planned improvements and future research priorities.

DSCIM-Coastal Impacts Modeling Hierarchy
DSCIM - Multi-sectoral Data-driven Spatial Climate Impact Model described in (Rode et al., 2021)
DSCIM-Coastal - Open-source platform for computing global coastal impacts, presented in this paper
SLIIDERS - Coastal segment datasets
SLIIDERS-ECON - Physical coastal characteristics and socioeconomic growth projections
SLIIDERS-SLR - Local relative sea level rise projections
pyCIAM - Global decision-modeling and projection system using *SLIIDERS* to model coastal impacts, based on CIAM (Diaz, 2016) and implemented in Python (v3.9)

Table 1. The major elements comprising the Coastal portion of the Data-driven Spatial Climate Impact Model (DSCIM-Coastal)

https://doi.org/10.5194/egusphere-2022-198
Preprint. Discussion started: 6 May 2022

2 Methods and Data

We constructed the Python Coastal Impacts and Adaptation Model (pyCIAM) by adapting the original code and structure of the Coastal Impacts and Adaptation Model (CIAM) (Diaz, 2016), obtained from http://github.com/delavane/CIAM in June 2020, with changes subsequently made in three phases:

1. Porting the model from GAMS to a standalone Python module (creating *pyCIAM*)
2. Updating all model inputs with the *SLIIDERS* data, constituting newer, improved physical and socioeconomic datasets
3. Implementing changes to the model functionality itself for the purposes of:
   - Computational efficiency
   - Updating assumptions where new data provided previously unavailable insights
   - Aligning model implementation with the model description in Diaz (2016)
   - Reducing noise in numerical approximation algorithms

2.1 Model Structure

The aspects of CIAM as presented in (Diaz, 2016) that are maintained in pyCIAM include the segment-based structure of the model and the adaptation actions that each segment is permitted to take throughout the modeling period, comprised of the following options:

- *Reactive Retreat*: When a portion of land falls below MSL, all people and mobile capital are relocated to an unaffected area, and immobile capital is abandoned.
- *Protection*: Construction of a generic levee to protect the entire coastline segment. Available choices for protection height include the 10, 100, 1000, and 10,000-year return values of ESL. This height changes linearly with RSLR.
- *Proactive Retreat*: All people and mobile capital below a certain retreat height are relocated to a safe elevation, and immobile capital below that height is abandoned. The options for that retreat height level are discretized to the same values available for protection, with the addition of a "low retreat" option representing the maximum MSL projected during a "planning period".

Note that, as described in Diaz (2016), each coastal segment may only choose one adaptation option, e.g. *retreat-1000*, for the entire model duration. While the height of the retreat level changes over time as the 1000-year ESL return value changes due to RSLR, the segment cannot, for example, choose retreat-100 for the first 40 years and then protect-10000.

The model is discretized into time steps (10 years in the original CIAM, annual in pyCIAM), during which all time evolving parameters are held constant. In addition, the segments use a configurable set of "planning periods", which each correspond to a set of one or more timesteps. For each planning period, a single height is chosen for retreat or protection (assuming the segment does not select "reactive retreat") that represents the maximum height projected for the chosen ESL return value during the planning period.

https://doi.org/10.5194/egusphere-2022-198
Preprint. Discussion started: 6 May 2022

2.2 Cost Calculation

Costs estimated by pyCIAM are categorized in the same manner as described in (Diaz, 2016).

2.2.1 Inundation Costs

The value of land and immobile capital lost to inundation. In Diaz (2016), immobile capital was allowed to fully depreciate if the strategy chosen is proactive retreat, such that capital-related losses due to inundation are always 0. This was based on a theoretical argument that for a planned retreat, a rational social planner would cease the creation of new physical capital far enough in advance that all remaining capital would have fully depreciated by the time the retreat occurs (Yohe et al., 1995). However, this assumption has been critiqued in subsequent work (Lincke and Hinkel, 2021) due to its lack of empirical grounding. Furthermore, it ignores the welfare loss associated with not replacing depreciating assets in the years leading up to retreat. These new capital investments would have been made in the absence of SLR, and thus the lack of investment should be counted when assessing total SLR impacts. Therefore, pyCIAM alters CIAM's assumption of full depreciation, instead modeling immobile capital to experience no excess depreciation beyond the background rate implicitly included in the capital growth model used to generate SSP-aligned capital projections. This results in the full estimated value of capital being lost when abandoned or inundated, in line with the assumptions of Lincke and Hinkel (2021).

2.2.2 Retreat Costs

The costs of relocating population and mobile capital and of demolishing immobile capital. Following Diaz (2016), capital relocation costs are valued at 10% of total value, and immobile capital demolition costs are valued at 5%. In Diaz (2016), the intangible relocation cost is valued at one year of per capita income, which varies by country and over time and was an admittedly arbitrary assumption. We use a value of five times local income, for reasons described in Sect. 2.3.

2.2.3 Protection Costs

The construction and maintenance costs of building a protective levee, along with the value of lost land. As in Diaz (2016), maintenance costs are assumed to be 2% of baseline costs, and the value of lost land is calculated as the local land value (which varies over countries and years) times the length and width of the barrier, assuming a 60° slope.

2.2.4 Wetlands Loss

The value of wetlands lost to either SLR or protection. As in Diaz (2016), wetlands are assumed to be able to partially absorb SLR up to 1 cm year^{-1}, with the degree of loss increasing quadratically with the rate of SLR. Above the critical threshold of 1 cm year^{-1}, all inundated wetlands are lost. In addition, all wetland area below a protective barrier is also assumed to be lost. More details on the calculation of wetland loss can be found in Equation 8 of the Diaz (2016) supplemental information.

https://doi.org/10.5194/egusphere-2022-198
Preprint. Discussion started: 6 May 2022

2.2.5 Extreme Sea Level Capital Damage

The value of capital loss occurring due to ESL events, using a depth-damage relationship that takes the shape $\frac{d}{1+d}$. The probability density function of ESL values at each segment location is represented as a Gumbel distribution, derived from Muis et al. (2016) in Diaz (2016) and from Muis et al. (2020) in pyCIAM. The product of this PDF and the estimated capital loss conditional on each ESL height in the distribution is integrated to obtain the annual expectation of ESL-driven capital loss per elevation slice, and these costs are summed over elevation to obtain the annual damages per segment (see Diaz (2016), Supplementary Material Section 2.1). For computational efficiency, this set of discrete products, integrations, and sums is performed on a variety of example inputs prior to executing the actual CIAM model. In Diaz (2016), functions are fit to these outputs to relate ESL height to loss for different adaptation options, with unique coefficients for each segment:

$$D_{r,s,t} = (1-\rho_{s,t})C_{s,t}\left(\frac{\sigma_{0,r,s}}{1+\sigma_{A,r,s}exp(\sigma_{B,r,s}H_{r,s,t})}\right) \quad (1)$$

$$D_{p,s,t} = (1-\rho_{s,t})C_{s,t}\left(\frac{\sigma_{0,p,s}+\sigma_{1,p,s}S_{s,t}}{1+\sigma_{A,p,s}exp(\sigma_{B,p,s}H_{p,s,t})}\right), \quad (2)$$

where

- $D_{r/p,s,t}$ is the ESL-driven expected capital loss conditional on retreat or protection to height r or p, respectively, for segment s in time step t,
- $\rho_{s,t}$ is a country-level resilience factor (defined in Diaz, 2016),
- $C_{s,t}$ is the capital density (in \$ per km^2),
- $H_{r/p,s,t}$ is the difference between the retreat or protection height and local mean sea level,
- $S_{s,t}$ is the local mean sea level, and
- σ are the fitted coefficients.

This has two notable issues. First, this fixed functional form may not fully represent heterogeneous relationships between adaptation height, MSL, and damage across segments, due to differing elevational distributions of capital at each segment. Second, only the protection equation contains a MSL term. This means that for retreat, ESL damages are modeled as constant relative to MSL, conditional on a fixed retreat standard (e.g. 1-in-10 year ESL height). This cannot be true unless capital is homogenously distributed over elevation. This assumption is at odds with reality and with the rest of the Diaz (2016) CIAM model, which assumes that the elevational distribution of capital follows that of land area.

In pyCIAM, we correct these issues by employing a multi-dimensional lookup table instead of these two functions. For each segment, we find the lowest and highest values of H and S across all SLR scenarios we wish to simulate, all adaptation choices, and all timesteps. We then choose 100 equally spaced values between these bounds for each of the two variables. For both of the adaptation categories (retreat and protection), we now have 10,000 scenarios. We normalize capital stock so that it sums to one, yielding fractional capital stock in each elevation slice. The current implementation assumes that these ratios remain fixed over time, though allowing for within-country population redistribution (e.g. Jones and O'Neill (2016)) could be accommodated by further indexing this lookup table by year. For each of the 20,000 scenarios, we calculate damages under a

https://doi.org/10.5194/egusphere-2022-198
Preprint. Discussion started: 6 May 2022

$\rho = 0$ assumption using a discrete double integral over ESL height and elevation slice. This yields damages for 10,000 unique combinations of H and S, for both retreat and protection options. In the pyCIAM model, the equations for damage are thus:

$$D_{r,s,t} = (1 - \rho_{s,t}) K_{s,t} \gamma(H_{r,s,t}, S_{s,t}) \quad (3)$$

$$D_{p,s,t} = (1 - \rho_{s,t}) K_{s,t} \gamma(H_{p,s,t}, S_{s,t}), \quad (4)$$

where $K_{s,t}$ is the total value of capital stock in segment s at time t and γ is the bilinear interpolation function across H and S, using the previously defined lookup table.

2.2.6 Extreme Sea Level Mortality

The expectation of annual VSL-valued costs of mortality occurring due to ESL events. Diaz (2016) estimates this by assuming 1% mortality for all populations exposed to a given ESL, based on Jonkman and Vrijling (2008). This is modeled similarly to the ESL-driven capital loss, except that the 1% mortality assumption is used in place of of the depth-damage function. In the implementation of Diaz (2016), the mortality assumption *and* the depth-damage function were used together. This is at odds with the description of the approach in the associated paper, and is thus corrected in pyCIAM.

2.2.7 Least Cost Optimization

For each planning period, every segment considers each of the possible adaptation options and assesses costs at each annual time step within the period. Like Diaz (2016), we maintain the assumption that these decision-making agents have perfect foresight of projected RSLR over this planning period; however, we reduce these periods from 40-50 years to 10 years (Sect. 2.7.2). The maximum heights of projected RSLR at each segment during a given planning period in turn influence the heights at which protect or retreat adaptation options are employed. Reactive retreat would match this projected RSLR and 10, 100, 1000, 10000-year retreat or protect actions would consider the heights of these ESLs atop the changing RSLR baseline for that planning period. Once adaptation costs are calculated for all adaptation periods, we follow (Diaz, 2016) and calculate the NPV across the entire model duration for each adaptation option, and each segment chooses the least cost option.[2]

2.3 Estimating Non-market Costs of Relocation

Diaz (2016) portrays the costs associated with "optimal adaptation" and "reactive retreat only" scenarios as bounds on future costs. This is justified by the observation that coastal adaptation at present does not appear to be economically rational, such that populations do not relocate or protect themselves when it seems optimal to do so (McNamara et al., 2015; Armstrong et al., 2016; Haer et al., 2017; Bakkensen et al., 2018; Hinkel et al., 2018; Suckall et al., 2018). This observation could be explained by uncaptured non-market costs of relocation associated with, for example, non-pecuniary emotional consequences. Accounting for these impacts would indicate that the total welfare impact of forced relocation is greater than the market costs associated with simply abandoning immobile capital.

[2] In contrast to Diaz (2016), we include initial adaptation costs from the first planning period in this NPV calculation (Sect. 2.7.3).

https://doi.org/10.5194/egusphere-2022-198
Preprint. Discussion started: 6 May 2022

Though CIAM partially represents non-market costs associated with moving, the model does not re-create observed patterns of settlement when it is initialized and run under an optimal adaptation scenario. Instead, it results in an excess of instantaneous relocation, suggesting that these non-market costs may not be fully represented. Specifically, when the optimal adaptation scenario is run under the baseline parameterization in Diaz (2016) and with the assumption of no climate-driven sea level rise, we observe that $1.26T of capital and 33M people instantly relocate. Adjusting for population and capital growth over the century, this instant relocation represents 41% and 44% of the *cumulative* relocation realized by the end of the century under the median SLR scenario for RCP 4.5. This large amount of instantaneous relocation clearly conflicts with the observed distribution of people and capital and suggests that there may be larger costs of relocation than are realized in the parameterization of CIAM used in Diaz (2016).

Diaz (2016) assumed these non-market costs are equal in value to consumption of one year of local GDP per capita, based on this value falling between two alternative estimates: 0.5 years (obtained from the author's personal communication with Robert Mendelsohn) and 3.0 years, the value assumed in the FUND Integrated Assessment Model (Tol, 1996). In a similar modeling framework, Lincke and Hinkel (2021) used the FUND value directly and further provided a literature review that finds empirical and theoretical estimates of total relocation costs varying between 2.3 and 9.5 years of average local income per capita. These empirical findings suggest that the factor of one used in Diaz (2016) may underestimate relocation costs.

To address this, we adopt an approach to calibrate these unobserved non-market costs of relocation against real world behavior. Our calibration approximates a "revealed preference" approach, in which the behavior of agents is thought to reveal information about their preferences and values that is not otherwise visible (other elements of DSCIM adopt related methods to estimate the undocumented costs of adaptation decisions in other sectors, e.g. see Carleton et al. (2020)). Intuitively, this strategy relies on the insight that if individuals found the benefits of moving to be larger than the combined market and non-market costs, they would relocate. We cannot observe the non-market costs, but we can estimate the benefits and the market costs. If we observe that individuals have not relocated but CIAM computes that the benefits outweigh the market costs even before considering SLR, then we can estimate a lower bound on the implied non-market costs (equal to the benefits minus the market costs) that must be present in order to prevent them from relocating and rationalize their observed behavior.

Our ability to constrain non-market costs using a revealed preference approach is constrained by our ability to accurately model benefits and market costs of relocation. There are inherent limitations in a global model (e.g. input data inaccuracies, preference heterogeneity) such that, at a segment-level, there will likely be some segments where benefits and/or market relocation costs are not measured exactly. Thus, we choose a relocation cost parameter by taking the exposure-weighted median value of segment-specific estimates of non-market costs.

To do this, we identify the total population and physical capital that would instantaneously relocate when the model is initialized in the absence of non-market relocation costs, assuming median estimates of RSLR in a no-climate change scenario (i.e., no change in GMSL, and RSLR associated only with land subsidence). For this simulation, we choose middle-of-the-road socioeconomic projections characterized by SSP2 and the International Institute for Applied Systems Analysis (IIASA) GDP growth model (Crespo Cuaresma, 2017). We then steadily increase the relocation cost parameter until 50% of that population and capital no longer instantaneously relocates under the optimal adaptation scenario. This median approach balances the

https://doi.org/10.5194/egusphere-2022-198
Preprint. Discussion started: 6 May 2022

desire to capture the non-market costs causing observed non-relocation with the recognition that data and parameter limitations associated with a global model will inevitably cause some seemingly irrational discrepancy between modeled and observed behavior. Because this median occurs at different values for population and physical capital, we average the two values (3.0 and 7.0 years of local income, respectively) to obtain the 5.0 factor used in pyCIAM. Fig. 1 illustrates this calculation.

We note that this approach is facilitated by the data fidelity represented in SLIIDERS and resolution provided by pyCIAM. The DIVA inputs used in Diaz (2016) assumed homogeneous population and capital density within each segment. This could introduce substantial noise in the elevation distribution of the observed present-day state of these two variables and would prohibit the analysis described above. By leveraging global gridded datasets of population, capital, and elevation, SLIIDERS and pyCIAM capture heterogeneous density and better represent the true present-day elevation distribution of population and capital within each segment (Sects. 2.6.1, 2.6.3, and 2.5.3).

After updating the non-market cost parameter, we additionally follow the approach of Lincke and Hinkel (2021) and do not distinguish between the non-market costs of reactive and proactive retreat. Diaz (2016) assigns five times higher costs to reactive retreat, though there is no empirical basis reported for this additional cost. Thus, both proactive and reactive retreat in pyCIAM incur losses equivalent to five years of income, rather than one and five years, respectively, in Diaz (2016).

2.4 Porting CIAM from GAMS to Python

CIAM was constructed in the closed-source General Algebraic Modeling System (GAMS) language. However, the model does not require the dynamic programming capabilities offered by GAMS. Therefore, porting the model to Python, a commonly used, open-source programming language, offers greater flexibility, access, and efficiency without loss of functionality. Before adding additional resolution to the model, pyCIAM computed a global run of a single SLR trajectory in 15-20 seconds, compared to 6-8 hours for CIAM. To ensure that this first stage of changes did not introduce changes to model functionality, we ensured that this version of pyCIAM replicated the results from the CIAM (in GAMS) model obtained from its source repository before updating model inputs. This replication was largely confirmed, with only very minor deviations between the computed results and those reported in (Diaz, 2016). The observed deviations were also reflected in the outputs of the unaltered CIAM model we obtained, suggesting that the configuration of the publicly available CIAM model was likely slightly altered from that used in Diaz (2016) (Table 2).

2.5 Physical Model Inputs in SLIIDERS

2.5.1 Coastal Segments

To improve the traceability of data inputs and the efficiency of model optimization, we replaced the irregular DIVA coastal segments with segments based on the Coastal Dataset for the Evaluation of Climate Impacts (CoDEC), a roughly uniform, 50-km spacing of global coastline points (Muis et al., 2020). We made a number of slight alterations to the original CoDEC point set and use these points as midpoints of 50-km coastline segments (Sect. A). The alterations ensured that (a) the coastline segments were nested by country boundaries, as the DIVA segments are, and (b) any extra points corresponding to offshore

https://doi.org/10.5194/egusphere-2022-198
Preprint. Discussion started: 6 May 2022

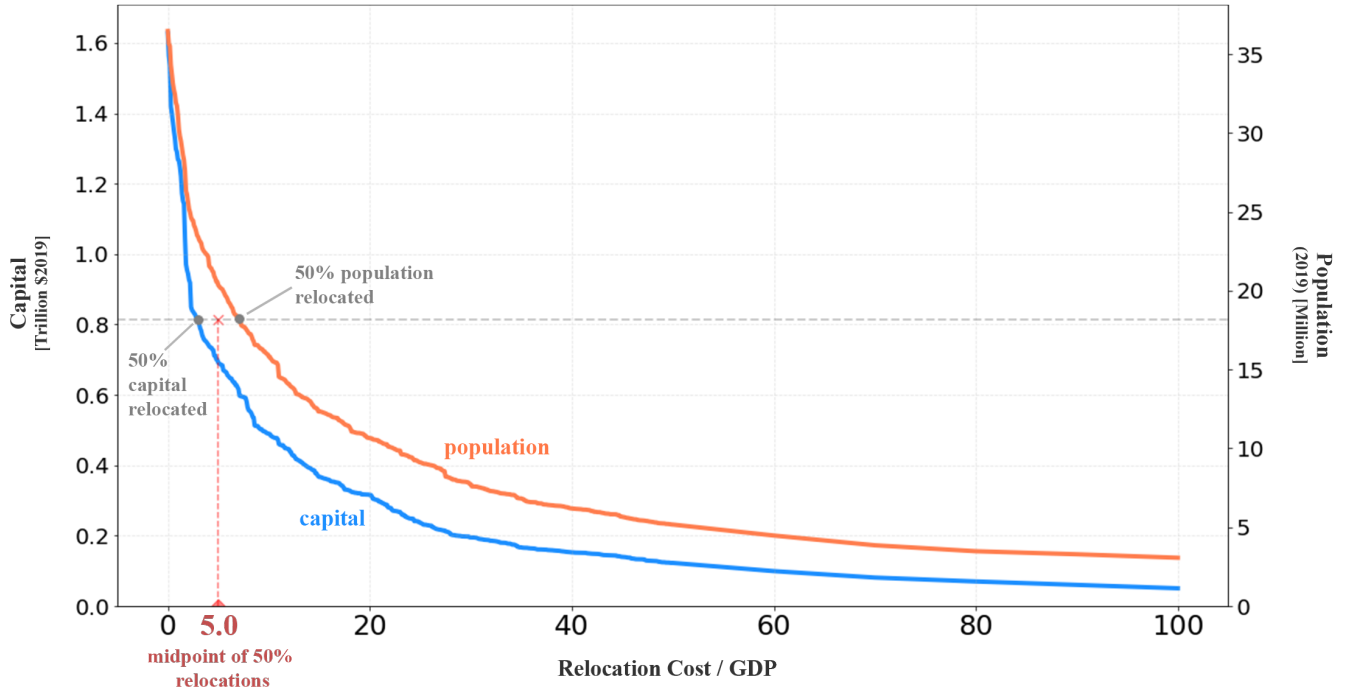

Figure 1. Estimation of the non-market relocation cost parameter through revealed preference. Curves show the magnitude of the population (blue) and physical capital(green) that is instantaneously relocated in the optimal adaptation scenario of pyCIAM, assuming SSP2-IIASA socioeconomic projections and median no-climate change RSLR, as a function of this parameter. The parameter is normalized by local GDP per capita. We identify the parameter values for which 50% of the population and capital instantaneously relocated under an assumption of zero non-market costs is no longer relocated, and average these two values to estimate the relocation parameter used in pyCIAM.

buoy gauges (used for validation in CoDEC) were removed. We also thinned European CoDEC points, originally provided at an extra fine 10km spacing, to 50km in order to have globally uniform spacing. We also manually added 15 segments for small island states or small slivers of national coastlines not represented in the original CoDEC point set (e.g. Anguilla, Tokelau, Jordan's small coastline, etc.). The final subset of CoDEC coastal points utilized in pyCIAM totaled 9,087. Natural Earth coastlines were used to make the point-to-segment conversion (1:50m resolution for the majority of segments and 1:10m for small island segments unresolved at coarser resolutions). The coastline lengths of each segment, used to calculate the potential costs of building protective barriers, were derived from this final set of segments (Sect. A1).

The decision to replace the coastal segments was motivated by several reasons. First, in the version of DIVA (v1.5.5) used in Diaz (2016), we found that many of the coastal segment lengths in high latitude regions were substantially overestimated, likely due to a geographic projection error. This error looked to be corrected in versions of DIVA used in subsequent studies; however, we nevertheless wished to avoid dependence of pyCIAM on DIVA, with uncertainty surrounding its ongoing development support and dataset availability. Second, we found that DIVA contains a substantial over-representation of small, mostly unpopulated land masses in island regions within its set of 12,148 segments. For example, DIVA contains 1,316 individual

https://doi.org/10.5194/egusphere-2022-198
Preprint. Discussion started: 6 May 2022

Billion USD ($2010)	Diaz 2016 (paper results)	CIAM (GAMS)	pyCIAM
Global NPV (2010-2100)	1700	1692.2	1692.2
U.S. NPV (2010-2100)	419	419.7	419.7
Australia NPV (2010-2100)	208	208.6	208.6
Brazil NPV (2010-2100)	98	97.5	97.5
China NPV (2010-2100)	87	87.0	87.0
Wetland Loss in 2100	80	79.3	79.3
Global Costs in 2100 (optimal adaptation)	270	282.1	282.1
Global Costs in 2100 (no adaptation)	2200	2251.5	2251.5
Calculation runtime	-	6-8 hours	15-20 seconds

Table 2. Comparison of select model results as reported in Diaz (2016) with those calculated from the original CIAM code in GAMS obtained from its online source repository and those calculated by pyCIAM after porting CIAM to Python and before any additional changes. Values reflect median relative sea level rise projections from Kopp et al. (2014) under a high emissions scenario (RCP 8.5). Model runs were conducted on an Apple MacBook Pro laptop with a 2.8 GHz Quad-Core Intel Core i7 processor and 16GB of RAM.

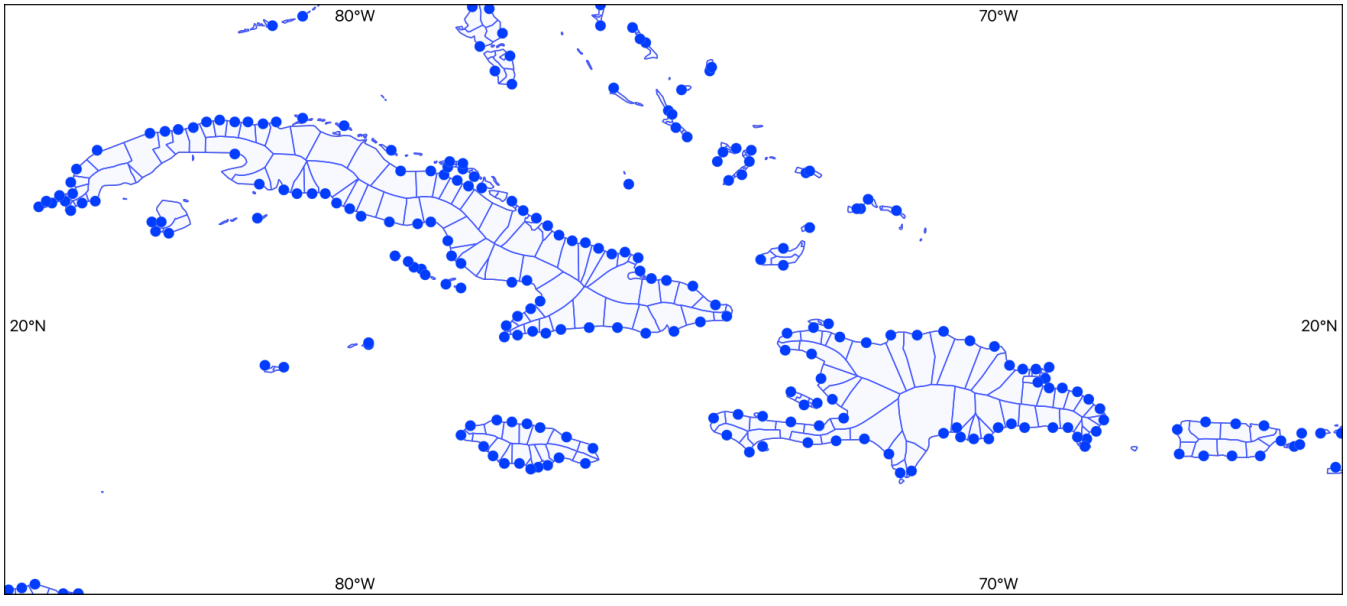

Figure 2. pyCIAM coastal segment centroids (points) and areas for a subregion of the Caribbean.

segments for French Polynesia, constituting 10.8% of all global segments despite representing less than 0.004% of global population. This created substantial computational inefficiencies, as all segments require roughly equivalent computation.

https://doi.org/10.5194/egusphere-2022-198
Preprint. Discussion started: 6 May 2022

2.5.2 Extreme Sea Levels

We obtained ESL distributions from CoDEC v1 (https://doi.org/10.5281/zenodo.3660927), which uses the third generation Global Tide and Surge Model (GTSM) combined with the ERA5 reanalysis to create a reanalysis product of historical sea levels (Muis et al., 2020). The CoDEC data provide the location and scale parameters of a Gumbel extreme value distribution fit to modeled ESLs at each coastline point, which we used to obtain the return periods required by CIAM (1, 10, 100, 1000, 10000-year). In validation analysis that compares CoDEC to observed tide gauge values, CoDEC values slightly underestimate annual ESL maxima by an average of 0.04m across all observed tide gauge stations, with 1-in-10 year mean ESL heights underestimated by 0.10m. Certain areas exhibit greater model bias, with 25% of tide gauge stations included in the validation showing absolute biases greater than 0.2m and 0.3m for annual and decadal maxima, respectively. In regions with large tidal range and/or frequent tropical cyclones, biases are generally larger. See Muis et al. (2020) for a full discussion of CoDEC model validity.

2.5.3 Elevation

The use of accurate elevation data is crucial to appropriately representing sea level rise impacts (Kulp and Strauss, 2019). We make three updates to the elevation model used to define the the population and physical capital exposed to SLR in pyCIAM:

1. We utilize the CoastalDEM v1.1 dataset (Kulp and Strauss, 2018) to define elevations at 1 arc-second resolution (roughly 30m). In addition to higher resolution elevation estimates compared to the 30-arc-second GLOBE DEM used in Diaz (2016), CoastalDEM significantly reduces bias found in previous DEMs. Compared to the widely used SRTM DEM, CoastalDEM suggests that roughly three times the amount of present day population resides below projected high tide levels under low emissions sea level rise scenarios by 2100 globally (Kulp and Strauss, 2019). It should be noted that the high-resolution version of CoastalDEM is the only input used in this study that is not publicly available. It is obtained via license with Climate Central, the developers of the DEM, though lower-resolution versions of the dataset are freely available for academic use. For the small number of regions we model where CoastalDEM does not exist (e.g. above and below 60N and 60S, respectively), we derive elevations from the SRTM15+ v2.3 dataset (Tozer et al., 2019).
2. We pair this DEM with our 30 arc-second population (LandScan 2019 (Rose et al., 2020)) and capital stock (LitPop (Eberenz et al., 2020)) rasters, which allows for independent calculations of the distribution of land area, capital, and population with respect to elevation. This differs from the approach used in Diaz (2016) where population and capital stock densities were defined at the segment level and assumed to be homogeneously distributed within a segment.
3. We discretize the distributions of population and capital to 0.1m elevation slices, rather than 1.0m.

2.5.4 Wetlands and Mangroves

For wetland areas, pyCIAM utilizes the European Space Agency's GLOBCOVER v2.3 global land cover dataset from 2009, offered at a 300m resolution (obtained in May 2021 from http://due.esrin.esa.int/page_globcover.php) (European Space Agency

https://doi.org/10.5194/egusphere-2022-198
Preprint. Discussion started: 6 May 2022

and UCLouvain, 2010). Three different land cover classifications from this layer, as defined in (Hu et al., 2017), were coded as "wetlands":

1. Closed to open ($> 15\%$) broadleaved forest regularly flooded (semi-permanently or temporarily) - Fresh or brackish water
2. Closed ($> 40\%$) broadleaved forest or shrubland permanently flooded - Saline or brackish water
3. Closed to open ($>15\%$) grassland or woody vegetation on regularly flooded or waterlogged soil - Fresh, brackish or saline water

Mangrove extents were updated using values from UNEP's Global Mangrove Watch 2016 dataset (Bunting et al., 2018) (obtained from https://data.unep-wcmc.org/datasets/45 in May 2021). The final wetland area used in pyCIAM consists of the spatial union of these two datasets.

2.5.5 Sea Level Rise

We use the LocalizeSL framework (Kopp et al., 2014, 2017) (https://doi.org/10.5281/zenodo.6029807) to "localize" probabilistic estimates of global SLR under a variety of assumptions of future global SLR and of the physical dynamics driving global ice sheet loss, similar to the approach taken in Sweet et al. (2017). Accounting for each of these different assumptions better captures structural uncertainty in how a given amount of global SLR will result in a particular spatial pattern of local SLR.

The computational improvements included in pyCIAM enable the application of the model to large probabilistic ensembles of SLR scenarios. Specifically, we apply the model to 110,000 Monte Carlo draws of SLR trajectories generated from LocalizeSL. These draws correspond to 10,000 draws each from 11 input scenarios:

- RCP 2.6, 4.5, and 8.5 projections from Kopp et al. (2014), as used in Diaz (2016),
- these same RCPs paired with different models of Antarctic ice sheet loss from DeConto et al. (2021) and Oppenheimer et al. (2019), and
- two non-RCP scenarios using Structured Expert Judgment to quantify the magnitude of contributions from global ice sheet loss to global SLR under a world in which global mean surface temperature stabilizes in 2100 at either 2°C or 5°C above pre-industrial temperatures in 2100, respectively (Bamber et al., 2019).

Each of these 11 scenarios corresponds to particular assumptions about future emissions and the contributions of ice sheets to SLR. At the high end of these projections, contributions from poorly constrained ice sheet instability could drive total GMSL rise approaching 2 m (Bamber et al., 2019; DeConto et al., 2021; Fox-Kemper et al., 2021).

Each of the 10,000 draws within each scenario corresponds to an equally likely realization of global and local SLR trajectories, conditional on those assumptions. For the purposes of this paper, we present results from each of these different SLR scenarios that correspond to the median draw at each coastal segment. In other words, the results for each SLR scenario reflect the impacts experienced by each segment in a world in which the emissions and ice sheet dynamics of that scenario play out, and each region of the world experiences the median projected RSLR for that scenario.

https://doi.org/10.5194/egusphere-2022-198
Preprint. Discussion started: 6 May 2022

In addition, similar to Diaz (2016), we run a "no climate change" scenario in which all SLR components are set to 0 except for a spatially heterogeneous background rate of change parameter that includes drivers assumed to be unaffected by climate change (e.g. glacial isostatic adjustment, tectonics, sediment compaction, and other processes contributing to vertical land motion). This is a probabilistic parameter in the LocalizeSL framework that is held fixed across the 11 scenarios. Within each scenario draws from the "no climate change" scenario are matched to those from the 11 "climate change" scenarios such that each group of 12 draws experiences the same non-climatic rates of RSLR.

2.6 Socioeconomic Variables

2.6.1 Population

In SLIIDERS, we use information from LandScan 2019 (Rose et al., 2020) to represent the present-day spatial distribution of population, scaled such that the aggregated country level population estimates match the 2019 estimates contained within the Penn World Table (PWT) v10.0 (Feenstra et al., 2015). In pyCIAM, we then maintain this within-country distribution and scale the country totals to match the SSPs (Riahi et al., 2017), exponentially interpolated between bi-decadal projections to annual values. Because the SSPs begin in 2010 and pyCIAM, like Diaz (2016), begins in 2000, we must scale populations back to 2000. To do so, we use observed country-level growth rates from 2000 to 2010 and apply these to SSP2 to estimate an initial population that is used for all SSPs in 2000. Observed rates are drawn from PWT, with missing countries filled by the 2019 UN World Population Prospects (UN DESA, 2019). For countries and territories not covered by the SSP data, we use global average population growth rates.

2.6.2 GDP

pyCIAM combines SSP-consistent, country-level GDP projections (from IIASA and OECD) and population projections (from IIASA) to create projected country-level income (i.e., GDP per capita) values (Riahi et al., 2017). SSP interpolation and extrapolation approaches match those used for population values. For the countries and territories not covered by IIASA and OECD projections, we take the global-average income in 2010 and interpolate/extrapolate using the global average yearly growth rates for missing years.

While we do not use historical GDP directly in the pyCIAM workflow, we utilize it in deriving the initial 2010 country level capital stock values; the methodology is described in Sect. A3. For this, we primarily derive historical national GDP levels between the years 1950 to 2020 from PWT 10.0. For countries and territories not covered by PWT 10.0, this data is augmented by multiple sources in a specified order of preference. These sources, in order, are the World Bank World Development Indicators (Bank, 2021), the 2021 IMF World Economic Outlook (IMF, 2021), the Maddison Project database (Bolt and van Zanden, 2020), OECD regional statistics (for Economic Cooperation and Development, 2020), the CIA World Factbook (Agency, 2021), various national account information sources, and academic papers (Treadgold, 1998, *Pacific Economic Bulletin*; Treadgold, 1999, *Asia Pacific Viewpoint*). Any remaining missing historical values of income and GDP per capita were imputed using income growth rates (further detail in Sect. A3).

https://doi.org/10.5194/egusphere-2022-198
Preprint. Discussion started: 6 May 2022

To create per capita income estimates (*ypc*) for coastal segments in pyCIAM for each year (t), we use the same national-to-segment downscaling approach as Diaz (2016), which assumes that urban coastal areas tend to have higher incomes than national average incomes, as follows:

$$ypc_{t,\text{segment}} = ypc_{t,\text{country}} \max\left\{1, \left(\frac{\sigma_{t,\text{segment}}}{250}\right)^{0.05}\right\} \quad (5)$$

where σ represents population density, in people per square kilometer, at the segment level. The 250 value is a population density constant that signifies an assumed dividing threshold between urban and rural areas and the income elasticity value of 0.05 is based on a regression presented in Lagerlöf and Basher (2005). In Diaz (2016) population density is assumed to be homogeneous within segment, and thus all elevation slices are prescribed the same local income. In pyCIAM, each elevation slice within each region has a unique population density. Thus, we apply this downscaling approach separately to each elevation slice.

2.6.3 Physical Capital

In addition to assessing the exposure of human population to SLR-related hazards, pyCIAM also assesses the exposure of physical capital stock to these threats. Both the IIASA (Crespo Cuaresma, 2017) and OECD (Dellink et al., 2017) GDP growth models utilize projections of capital growth; however, neither model has publicly released these projections. Therefore, to create future capital stock estimates, we extract the capital relevant growth equations for the OECD's Env-Growth model as described in Dellink et al. (2017). The capital growth trajectory in the IIASA model is exogenously specified, constant across SSP scenario, and yielded implausibly large capital stocks in later years. For instance, the IIASA model projects that Macau experiences a capital growth rate of 14% per annum from 2010 to 2100. This trajectory implies that Macau reaches $30.8 quadrillion in 2100 capital stock, which is 23 times that of the U.S. in 2100 ($1.3 quadrillion) and 200,000 times that of Macau in 2010 ($134 billion) (all values in constant 2019 PPP USD). Due to such implausible growth rates, we do not use the IIASA capital growth trajectory in pyCIAM.

We use country-level 2010 capital stock information from PWT 10.0 (Feenstra et al., 2015) as the initial conditions for this growth model. For the countries not represented in PWT 10.0 (Feenstra et al., 2015), pyCIAM combines physical capital data from Global Assessment Report (GEG-15) (Bono and Chatenoux, 2014) and LitPop (Eberenz et al., 2020) (for the years 2005 and 2014, respectively), historical GDP values, and methods from Higgins (1998) and Inklaar et al. (2019) to estimate 2010 capital stock. Then, we apply the OECD capital stock equations with the estimated 2010 capital stock values and SSP-consistent GDP projections to obtain projections of capital stock for each SSP scenario and for each GDP growth model. To parameterize these equations, we use a value for the partial elasticity of GDP with respect to capital taken from Crespo Cuaresma (2017) (0.326), since this is not reported in Dellink et al. (2017). We also estimate country-specific initial conditions for the marginal product of capital using a modified Cobb-Douglas production function fit to the historical capital and income data. See Sect. A3 for further methodological detail.

pyCIAM uses the LitPop dataset (Eberenz et al., 2020) to represent within-country spatial distribution of physical capital stock at 30 arc-second resolution. LitPop combines population information from the Gridded Population of the World dataset

https://doi.org/10.5194/egusphere-2022-198
Preprint. Discussion started: 6 May 2022

(v4.1) (University, 2016) with nightlight intensity (Román et al., 2018) to downscale country-level estimates of total physical assets. In some countries, e.g. Libya and Syria, LitPop does not provide any downscaled estimates. In these locations, we use the downscaled estimates provided by the GEG-15 dataset (Bono and Chatenoux, 2014).

In pyCIAM, the ratio of mobile to immobile capital is used to determine costs of inundation. Diaz (2016) used a fixed ratio of 10%. However, PWT 10.0 contains country-level information that can be used to estimate across-country heterogeneity in this ratio. PWT decomposes physical capital into four categories:

- Residential and non-residential structures
- Machinery and non-transport equipment
- Transport equipment
- Other assets

For SLIIDERS, we assume that the first category (residential and non-residential structures) represents immobile capital and the others represent mobile capital. We take the average mobile fraction from 2000-2019 and apply this at the country level. These country specific values vary from 1% (Haiti) to 52% (Equitorial Guinea) with 25th, 50th, and 75th percentiles of 14, 18, and 20%, respectively.

2.6.4 Construction Costs

We maintained the same reference unit cost of coastal protection utilized in CIAM but updated the national construction cost index scaling factors by using the ratio of construction cost indices from ICP 2017 (World Bank, 2020) instead of 2011. For countries not included in this dataset, we augment with the country-level construction cost indices used in Lincke and Hinkel (2021), averaged across the rural and urban distinction.

2.7 Other Features

2.7.1 Model Duration

Diaz (2016) runs from 2000-2200. However, the SSPs stop at 2100 and thus the SLIIDERS-ECON dataset does as well. Because of this, we limit pyCIAM to 2000-2100. Using the 4% discount rate employed in Diaz (2016) and pyCIAM, the discount factors for 2100-2200 costs vary from 2% in 2100 to 0.04% in 2200, so the exclusion of these additional years is unlikely to have a substantial effect on the optimal adaptation option selected by each segment.

2.7.2 Timesteps and Planning Periods

We increase temporal resolution from the decadal timesteps used in Diaz (2016) to annual. In addition to the exponential interpolation of bi-decadal SSP inputs, described above, decadal SLR projections are linearly interpolated to yield annual values. The 40-50 year planning periods used in Diaz (2016) yield substantial step-changes in realized costs at mid-century and end-of-century due to substantial simultaneous global adaptation actions. To generate a smoother time series of costs, we use decadal planning periods. A potential trade-off of using shorter planning periods is that this may overestimate the frequency

https://doi.org/10.5194/egusphere-2022-198
Preprint. Discussion started: 6 May 2022

with which governments and populations are able to update major adaptation actions. An unrealistically agile representation of large-scale adaptation actions may underestimate associated costs. Future work may empirically estimate the frequency at which adaptation approaches are updated and explore further options for incorporating planning periods that are not globally simultaneous and thus do not lead to step-changes in global SLR costs at the start of each period.

2.7.3 Net Present Value Calculation

In pyCIAM, the NPV each segment uses to calculate an optimal adaptation approach is calculated from 2010-2200, excluding the initial planning period of 2000-2009. In this way, each segment is allowed a "free" initial relocation or protection action. For example, if a segment chooses to protect to the 1-in-10,000 year ESL height, which is 3 meters, they do not consider the costs of building a corresponding seawall when calculating the NPV of this action. They only consider the marginal cost of extensions to this seawall to remain at the 1-in-10,000 year height as local sea levels increase. This is not reflective of the full costs of relocation or protection. Thus, in pyCIAM, we include these initial costs in the NPV calculation, using the entire model duration of 2000-2100.

In addition, Diaz (2016) applied the discount rate at the start of each decadal timestep to the full 10 years of costs incurred in that timestep. We avoid this issue by using annual timesteps; however, when comparing NPV results to Diaz (2016) (Fig. 5), we apply annually varying discount rates to the Diaz (2016) outputs as well.

2.7.4 Observed Present-Day Protection

In Diaz (2016), no observed protection standards were included. In pyCIAM, we use the National Levee Database (US Army Corps of Engineers) to define protected areas in the U.S. and we assume that all population and capital stock in the Netherlands is protected due to the country's massive "Delta Works" project. All population, capital, and land area within these areas are excluded from SLIIDERS-ECON and from the pyCIAM model. Future work will increase the spatial coverage and improve the representation of present-day protections.

2.7.5 Manual Correction Factors

In pyCIAM, the following manual correction factors in the original code underlying Diaz (2016) have been removed. These correction factors were originally used by Diaz (2016) in order to correct for certain limitations in data availability or quality that are no longer necessary after incorporating the data updates in SLIIDERS:

- Doubling the price of construction on all "island" segments. The new construction cost index values utilized in pyCIAM should theoretically capture any increased construction costs on island nations. Additionally, segments defined as "island" in CIAM were not entirely consistent, with some islands receiving the label and others not.
- Halving the protection heights under the protection adaptation scenario corresponding to 10-year ESL heights. This was originally implemented to account for elevation profiles found in the GLOBE DEM that were deemed physically im-

https://doi.org/10.5194/egusphere-2022-198
Preprint. Discussion started: 6 May 2022

plausible (extremely high area totals from 0-1m), but is no longer required following the updated CoastalDEM elevation values.

– Averaging of the inundated land area-by-elevation bins for the first two (0-1m, 1-2m) bins in order to smooth the elevation profile due to the high 0-1m area totals in the GLOBE DEM values. This adjustment, too, is no longer required following the updated CoastalDEM elevation values.

3 Results and Discussion

Upon implementing the changes described above, global costs estimated by pyCIAM diverge from those in Diaz (2016). Additionally, we obtain estimates for a greater breadth of socioeconomic and emissions scenarios, using multiple assumptions of ice sheet instabilities to reflect deep uncertainty in these processes. Fig. 5 displays estimated global costs for the following global SLR-driven cost metrics reported in Diaz (2016): (i) end-of-century annual costs of wetland loss, (ii), end-of-century annual total costs under an optimal adaptation scenario, (iii) end-of-century annual total costs under a "reactive retreat only" scenario, and (iv) global net present costs using a 4% discount rate.

Results are shown for the pyCIAM model both in its replicated CIAM configuration and after all the above changes were applied. Values are expressed such that each vertical group of points comprise the spread of results between the different socioeconomic projections for a given SLR scenario, with the position along the x-axis representing that scenario's median GMSL value in 2100. As described in Sect. 2.5.5, all of the pyCIAM results use a constructed "median" SLR trajectory where each location experiences the median RSLR across the probabilistic projected distribution. This matches the approach in Diaz (2016), used to create the displayed CIAM results.

ID	SLR Scenario	Model Used	2100 median GMSL [m]
NCC	No Climate Change*	CIAM, pyCIAM	0.00
K14	Kopp et al. 2014 (RCP 2.6, RCP 4.5, RCP 8.5)	CIAM, pyCIAM	0.49, 0.59, 0.79
SR	IPCC-SROCC (RCP 2.6, RCP 4.5, RCP 8.5)	pyCIAM	0.49, 0.61, 0.89
B19	Bamber et al. 2019 (Low, High)	pyCIAM	0.69, 1.11
D21	DeConto et al. 2021 (RCP 2.6, RCP 4.5, RCP 8.5)	pyCIAM	0.53, 0.63, 1.11

*Includes local background rates of relative sea level rise at each segment due to non-climatic background processes.

Table 3. GMSL rise between 2000 and 2100 for each SLR scenario used in the pyCIAM and Diaz (2016) models, representing the x-axis positions of median costs by scenario displayed in Fig. 5.

https://doi.org/10.5194/egusphere-2022-198
Preprint. Discussion started: 6 May 2022

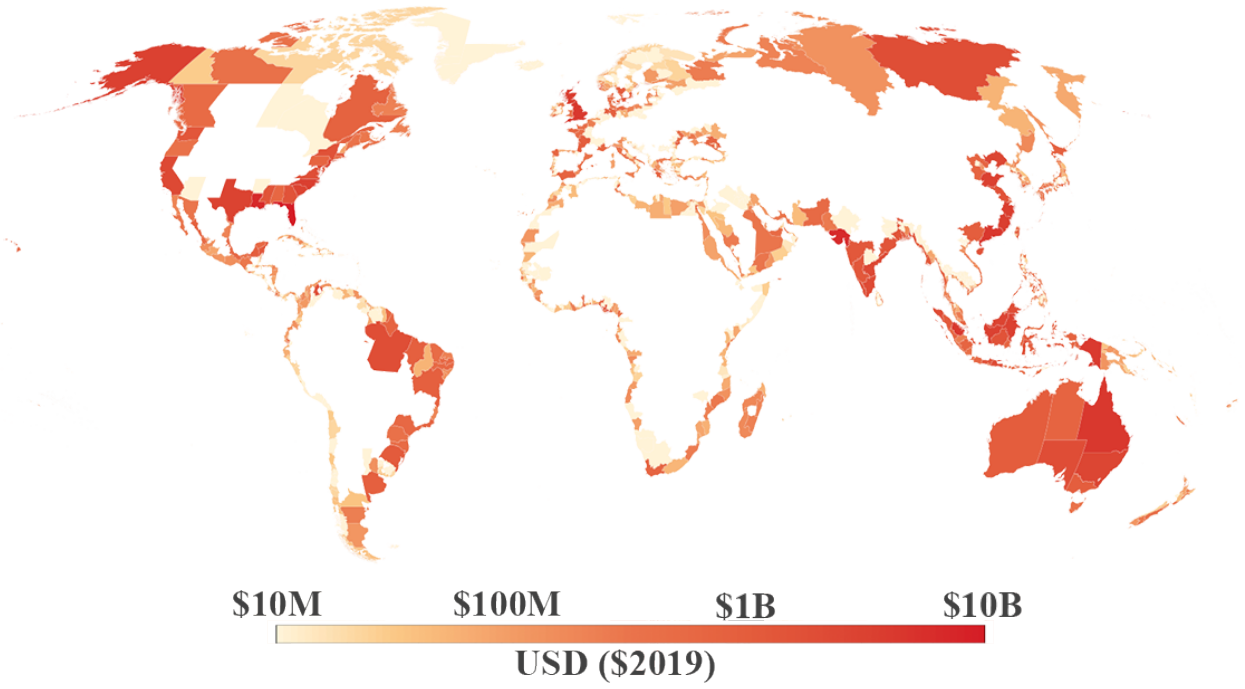

Figure 3. Estimated annual average costs in 2100 by "admin 1" region (equivalent to state-level in the U.S.). Results shown reflect optimal adaptation, using the IPCC - Special Report (SROCC - RCP 8.5) SLR scenario and SSP2/IIASA socioeconomic projections.

3.1 Total SLR Costs

The global distribution of end-of-century average annual costs of climate-driven SLR under optimal adaptation, aggregated to "admin 1" regions (equivalent to state-level in the U.S.), is shown in Fig. 3, using the SROCC-RCP8.5 SLR scenario and SSP2-IIASA socioeconomic trajectory. Fig. 4 similarly demonstrates spatial heterogeneity in the total benefits realized through optimal adaptation, relative to the "reactive retreat only" scenario.

Generally, global estimates of the SLR-driven costs of climate change in pyCIAM are similar to those of Diaz (2016) (Fig. 5). Median global NPV values from 2000-2100 under optimal adaptation ranges from $680 billion to $2.1 trillion in pyCIAM across its 110 SLR-SSP-IAM scenarios, corresponding to end-of-century GMSL rise values between 0.49 and 1.11m. Estimates of global NPV from Diaz (2016) range from $1.1 to $1.5 trillion in the three SLR scenarios considered (end-of-century GMSL rise from 0.49 to 0.79m, Table 3). Comparing the three SLR scenarios used in pyCIAM that match those employed in Diaz (2016) (K14 RCPs 2.6, 4.5, 8.5), pyCIAM's median global NPV values from 2000-2100 are generally slightly below those estimated by CIAM (Fig. 5, Table 4). However, when considering total damages under both the 11 "climate change" scenarios and the "no climate change" scenario, rather than the difference between them, pyCIAM estimates significantly higher global NPV (3-4x) and moderately higher end-of-century costs than Diaz (2016) (Fig. B1). This may be largely attributed to the fact

https://doi.org/10.5194/egusphere-2022-198
Preprint. Discussion started: 6 May 2022

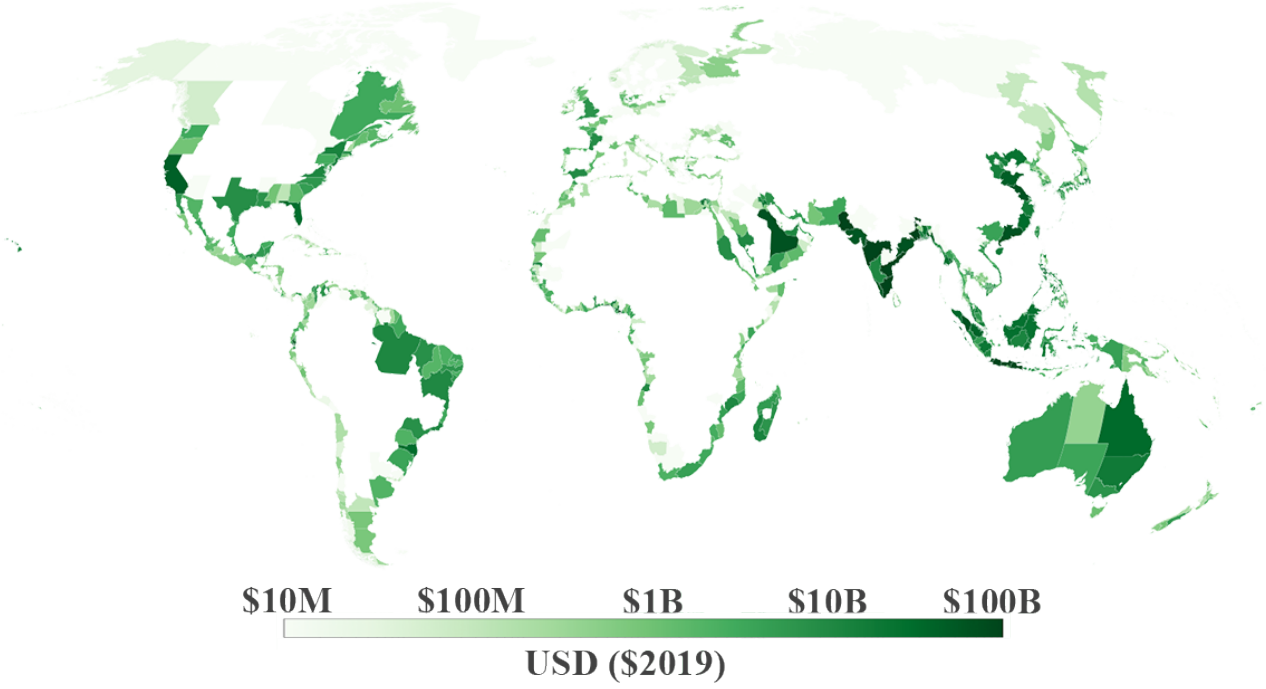

Figure 4. Estimated annual adaptation benefits in 2100 by "admin 1" region (equivalent to state-level in the U.S.). Results shown reflect the IPCC - Special Report (SROCC - RCP 8.5) SLR scenario and SSP2/IIASA socioeconomic projections.

that projected capital stock and population in SLIIDERS across its SSP and growth model scenarios are significantly higher than those modeled in Diaz (2016). For example, the mid-century global capital stock located between 0 and 15 meters above sea level ranges from $210 to $370 trillion (2019 USD) across the five SSPs and two growth models in SLIIDERS, compared to $97 trillion in Diaz (2016). Similarly, SLIIDERS' mid-century population ranges from 1.39 to 1.58 billion people, compared to 1.18 billion in Diaz (2016). The SSP-based ranges differ most from the Diaz (2016) trajectories around mid-century before beginning to converge toward end-of-century. This behavior aligns with the observation that end-of-century annual costs are more similar across pyCIAM and Diaz (2016) than total NPV.

Annual global costs due to SLR in 2100 under optimal adaptation range from $85 billion to $1.1 trillion across all pyCIAM scenarios, and from $85 billion to $590 billion across the K14-pyCIAM scenarios. The corresponding Diaz (2016) values range from $150 billion to $290 billion. Under "reactive retreat only", pyCIAM values generally exceed those of Diaz (2016) for all SLR scenarios (Fig. 5, Table 5).

3.2 Adaptation Costs and Benefits

The global distribution of optimal adaptation strategies is displayed in Fig. 6 for the SROCC-RCP8.5 SLR scenario and SSP2/IIASA socioeconomic scenario. Notably, the majority of segments that protect are located in Asia, where coastal popu-

https://doi.org/10.5194/egusphere-2022-198
Preprint. Discussion started: 6 May 2022

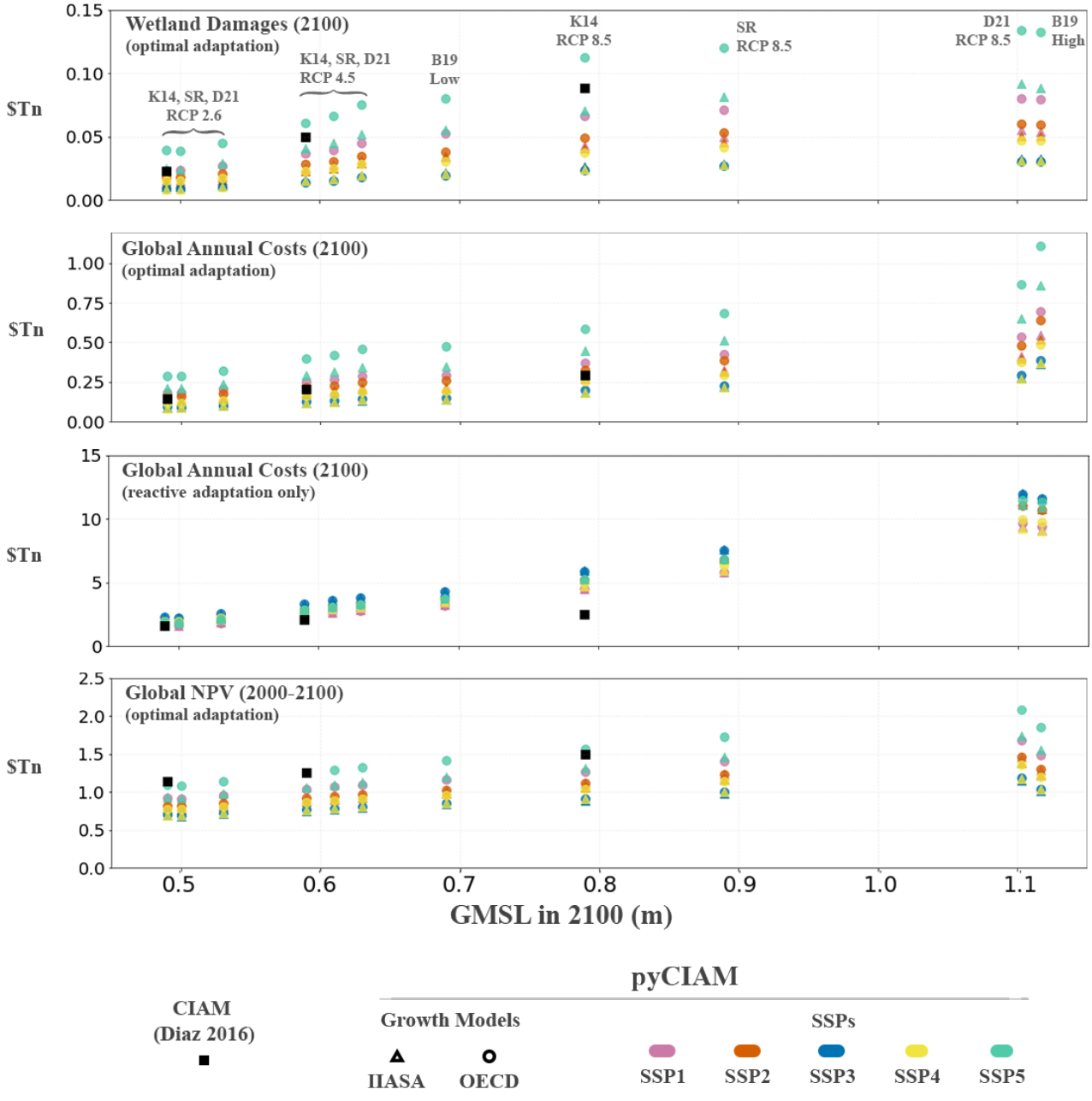

Figure 5. Comparison of four global cost metrics for median model results under each SLR scenario, for CIAM (black) and pyCIAM (colored). Values represent costs from climate change induced SLR only, i.e. after differencing the time series of costs under a "no climate change" scenario with median non-climatic RSLR rates and no GMSL rise. All costs are expressed in constant 2019 PPP USD. Each vertical group of points represents a single SLR scenario (Table 3), with each point in the group representing a unique combination of SSP and growth model. n.b. The D21-RCP8.5 and B19-High SLR scenarios share the same projected GMSL in 2100 (1.11m) and were jittered by +/- 0.007m for plotting clarity.

https://doi.org/10.5194/egusphere-2022-198
Preprint. Discussion started: 6 May 2022

NPV (2000-2100) $Trillion	pyCIAM (*min*)	pyCIAM (*max*)	CIAM (*min*)	CIAM (*max*)
Optimal Adaptation	0.680	2.08	1.14	1.49
Reactive Adaptation Only	2.66	11.9	6.07	8.41

Table 4. Range of net present costs of climate-driven SLR from 2000 to 2100 in constant 2019 PPP USD across all 110 socioeconomic and SLR scenarios. Minimum and maximum NPV values are shown for the fully updated pyCIAM model, as well as CIAM as configured in Diaz (2016).

End of Century Annual Costs $Trillion	pyCIAM (*min*)	pyCIAM (*max*)	CIAM (*min*)	CIAM (*max*)
Optimal Adaptation	0.0853	1.11	0.146	0.293
Reactive Adaptation Only	1.57	12.0	1.58	2.50

Table 5. Range of end-of-century average annual costs of climate-driven SLR from 2000 to 2100 in constant 2019 PPP USD across all 110 socioeconomic and SLR scenarios (for pyCIAM, paired with SLIIDERS inputs) and across three SLR scenarios (for CIAM).

lation densities are generally high and construction costs, at least as parameterized by CIAM and pyCIAM, are relatively low. Scattered high-density areas across OECD countries in Europe and North America are protected as well. The fact that most protecting segments opt for the maximum level of protection (1-in-10,000-year ESL height) also suggests that, for segments where protection is optimal, the marginal costs of building higher protection are almost always lower than the benefits they provide, up to the point where the protection heights have provided safety from an exceedingly rare event. Future work should further explore the empirical validity of the construction cost functions used in Diaz (2016) and ported to pyCIAM as these may control the spatial distribution of protection. Similar to the dominance of maximum protection, there is a common preference to retreat to the 1-in-10-year ESL height amongst segments that adopt retreat as their optimal strategy. This suggests that increasing the resolution of retreat options around this level may better reflect heterogeneity in optimal retreat height. Finally, segments for which reactive retreat is optimal are generally sparsely populated or unpopulated, as seen in the low percentages of global population residing in these segments (Fig. 7).

Fig. 7 displays the proportion of global segment populations adopting different adaptation strategies (protection, proactive retreat, and reactive retreat), across the various socioeconomic and SLR scenarios for both pyCIAM/SLIIDERS and CIAM. In general, while CIAM indicates that roughly 50% of the world's population would be protected under optimal adaptation and 50% would be relocated, pyCIAM, paired with SLIIDERS inputs, finds these ratios to be closer to 75% and 25%, respectively. This is primarily due to our increased relocation cost parameter (Sect. 2.3), which disincentivizes retreat relative to protection. In contrast to the influence of relocation cost on adaptation type, little variance is observed in these percentages across pyCIAM's different socioeconomic scenarios. This high stability is seen even within individual segments' adaptation choices and

https://doi.org/10.5194/egusphere-2022-198
Preprint. Discussion started: 6 May 2022

suggests that particular choices of adaptation strategy at a local level may often be robust to a range of future socioeconomic and SLR trajectories. Similar results are shown normalized by coastline length rather than population in Fig. B2.

3.3 Model Limitations and Planned Improvements

The benefits of adaptation presented here reflect the difference between costs in a scenario where only reactive SLR adaptation is allowed and one where all segments adapt optimally. However, "optimal" adaptation modeling in pyCIAM is subject to some of the same limitations as its predecessor CIAM. First, adaptation is limited to the ten possible options introduced in Diaz (2016) — four protection heights, five proactive retreat heights and a reactive retreat action. Second, segments are only allowed one protection or retreat standard throughout the model duration. They cannot, for example, retreat to the 1-in-10 year ESL height for the first 20 years and then retreat to the 1-in-100 year height, rather an optimal retreat timing and height is chosen given the full distribution of potential future outcomes. Segments also cannot retreat to a certain height and then protect from there. Third, insurance, subsidies or other policies may discourage proactive retreat even when the NPV would be positive, and these interventions are not taken into account by segment agents in the model. Fourth, many cost functions and parameters in the model are based on limited empirical evidence, as little evidence at fine resolution and global scale is available to inform the magnitude and heterogeneity of these costs. Fifth, existing coastal protections are not directly modeled at a global scale, though this is addressed for some regions such as the U.S. and the Netherlands (Sect. 2.7.4). Lastly, retreat or protection heights within each decadal planning period are chosen under perfect foresight of projected RSLR at that segment during the entire period, such that any maximum projected change in ESL return values due to RSLR is perfectly anticipated and incorporated into adaptation cost considerations and decisions. Notably, segments also chose their optimal adaptation strategy (e.g. protection to the 1-in-100 year ESL height) based on an NPV calculation that utilizes perfect foresight over the entire model duration. While this assumption cannot be correct in its extreme form, Fig. 7 suggests that these choices are very robust to uncertainty in future sea level and socioeconomic change.

Limiting possible protect and retreat heights to local 1, 10, 100, 1000, 10000-year ESL heights makes the range of adaptation heights dependent on the distribution of local ESL heights, which may artificially restrict options for modeled relocation or levee construction heights. Similarly, the model's current implementation does not allow for multiple adaptation strategies over the course of the modeling period. For example, a segment that chooses the 1-in-10 year protection height will continue to build higher protections as RSLR shifts the local ESL distribution, but it is not allowed to change to a greater protection standard (e.g. 1-in-100 year heights) or switch to retreat in the middle of the model duration. More flexible approaches may enable lower-cost outcomes (Kopp et al., 2019; Haasnoot et al., 2019), though computational constraints have limited the implementation of more dynamic adaptation approaches to models with local domains (Lickley et al., 2014). A preliminary approach to this problem, such as allowing for a one time, mid-century alteration of adaptation strategies, could be a simple scheme to allow for some level of dynamic adaptation strategies.

pyCIAM also does not currently represent accommodation measures (e.g., infrastructure hardening and building elevation), which in some cases may be more cost-effective than either protection or retreat Oppenheimer et al. (2019); Kopp et al. (2019); Rasmussen et al. (2020). Accommodation encompasses a broad range of actions and is thus difficult to parameterize within the

https://doi.org/10.5194/egusphere-2022-198
Preprint. Discussion started: 6 May 2022

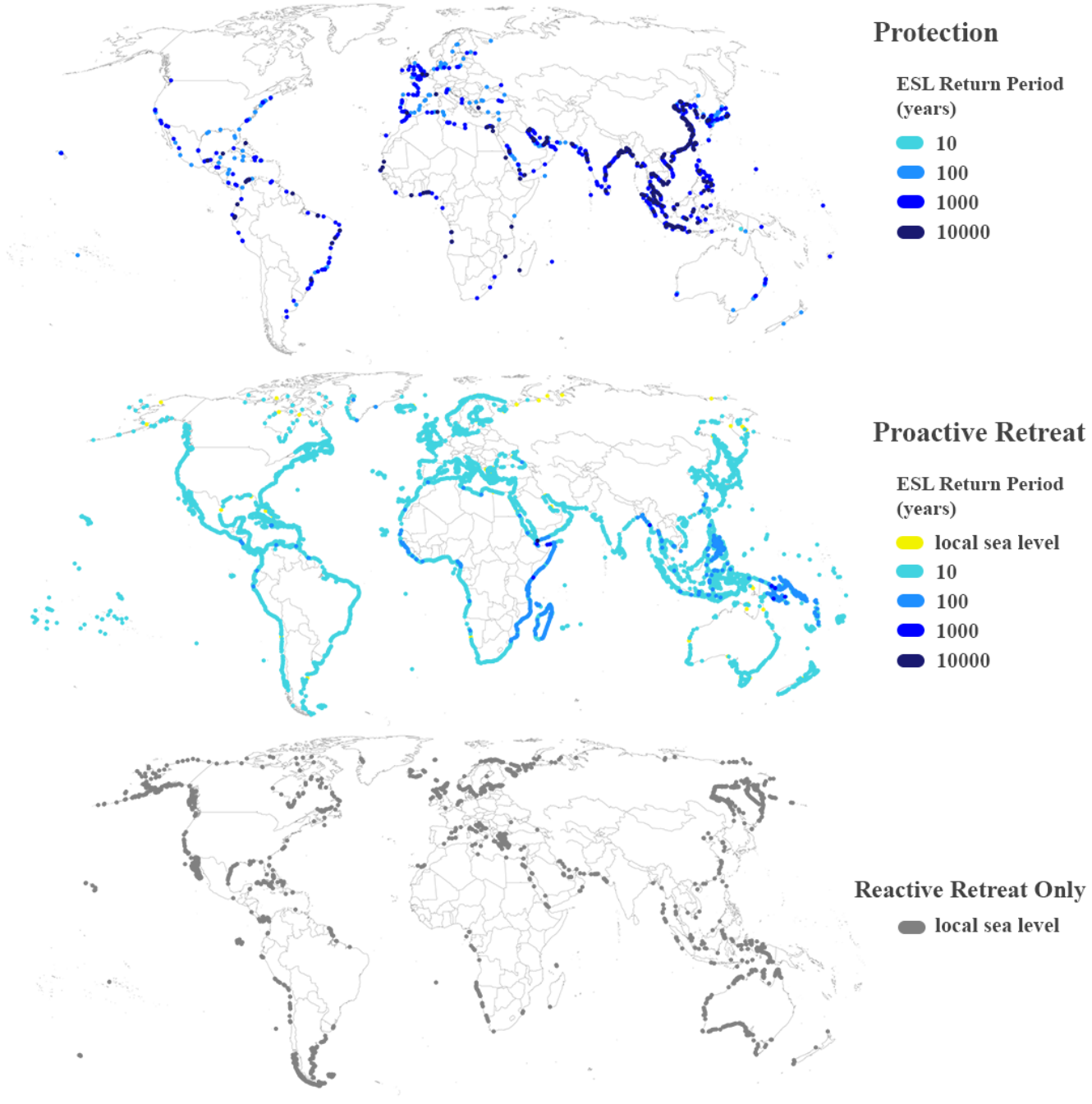

Figure 6. Adaptation strategies by each segment in the "optimal" adaptation scenario. Results reflect the IPCC - Special Report (SROCC - RCP 8.5) SLR scenario, SSP2 and IIASA growth model socioeconomic growth projections

https://doi.org/10.5194/egusphere-2022-198
Preprint. Discussion started: 6 May 2022

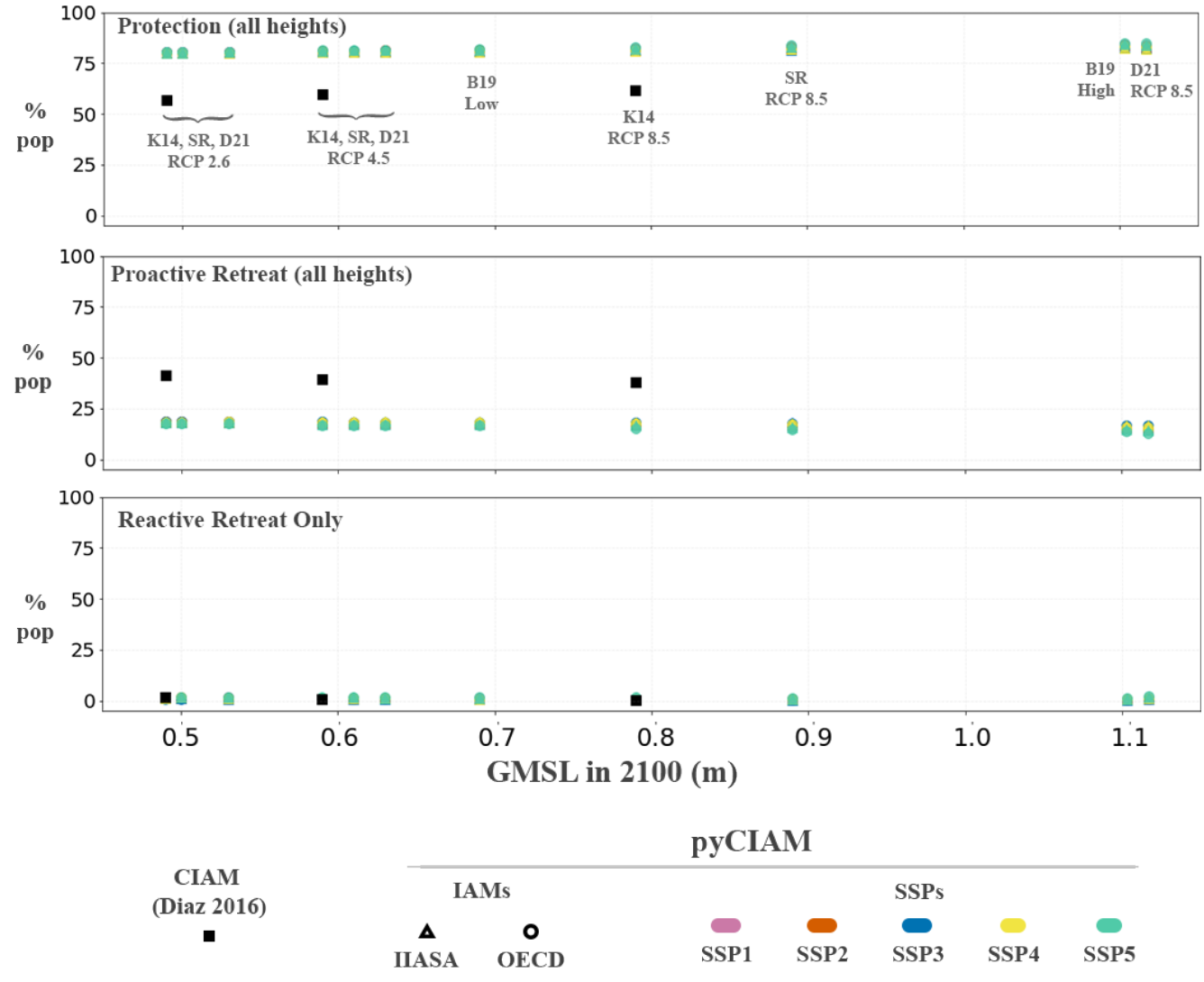

Figure 7. Comparison of optimal adaptation strategies adopted across all segments. Values represent percentages of global population at that reside below at elevations below 15 meters in segments adopting each respective adaptation strategy. Proactive retreat and protection values are aggregates of all possible heights for each. Solid black squares represent the results from Diaz (2016) and the colored circle and triangle markers represent pyCIAM/SLIIDERS results for all SLR (differentiated by GMSL values), SSP and growth model scenarios. n.b. The D21-RCP8.5 and B19-High SLR scenarios share the same projected GMSL in 2100 (1.11m) and were jittered by +/- 0.007m for plotting clarity.

https://doi.org/10.5194/egusphere-2022-198
Preprint. Discussion started: 6 May 2022

model. To our knowledge, accommodation is not represented in other coastal modeling platforms but could be the subject of future updates to pyCIAM.

Our current estimation of the non-market costs of relocation detailed in Sect. 2.3 is intended to represent the fact that many coastal areas are observed to currently be under-adapted to present ESL hazards (Houser et al., 2015; McNamara and Keeler, 2013; McNamara et al., 2015; Armstrong et al., 2016; Haer et al., 2017; Hinkel et al., 2018; Suckall et al., 2018; Lorie et al., 2020). However, improved estimates of these non-market relocation costs could potentially be guided by more detailed empirical assessments of present-day under-adaptation to coastal hazards. Other forms of adaptation behavioral "inertia" preventing or delaying economically rational action may exist as well. Mendelsohn et al. (2020) estimated the cost-benefit ratio of building seawalls to be at least 2:1 in East Haven, CT, Council (2017) estimates this ratio for elevating coastal homes up to 9:1 in some U.S. locations, and Bakkensen and Mendelsohn (2016) found that the U.S., in particular, may be up to 14x less adapted to tropical cyclone hazards than other OECD countries threats presently. While some of this under-adaptation is rationalized by our non-market costs of relocation, other factors such permitting and funding costly infrastructure projects, subsidized insurance (Craig, 2019) or limited risk information may play a role as well. We are aware of efforts to further understand adaptation costs and the reasons for under-adaptation (Bower and Weerasinghe, 2021; Berrang-Ford et al., 2021), but the current extent of empirical evidence quantifying sub-optimal adaptation is limited. If and when such evidence is available, the modularity of pyCIAM enables future integration of these estimates to improve its adaptation cost-benefit implementation.

Better global data describing existing coastal protection infrastructure would improve the accuracy of pyCIAM. Currently, the model incorporates coastal barriers that are well documented, such as seawall and levee systems in The Netherlands and the U.S. However, spatially resolved data on constructed protection around the globe is sparse. To overcome this, some studies assume a certain level of protection as being present in all coastal regions, making stylized assumptions based on population densities and national GDP (Sadoff et al., 2015). Other studies develop statistical models to empirically ground such relationships (Scussolini et al., 2016), and these have been incorporated in other global coastal adaptation models (Tiggeloven et al., 2020) and could be evaluated for use in future versions of pyCIAM. Further improvements to certain regions could also be made using protection data collected by Hallegatte et al. (2013) for 136 coastal cities.

4 Conclusion

Modeling the social and economic impact of future sea level rise can inform our understanding of costs in different climate change mitigation scenarios and support the analysis of adaptation policies. To construct global estimates, modelers face the dual challenge of developing a global approach capable of representing the detailed local information relevant to accurately estimating SLR impacts and adaptation. Prior modeling studies have developed valuable frameworks for conducting such analyses; however, continued iteration of these data and models is necessary in order to improve the accuracy and precision of projections and to keep pace with relevant advancements in data, modeling, and computing. Achieving this through community-wide collaboration requires a collection of open-source and transparent datasets as well as modeling tools.

https://doi.org/10.5194/egusphere-2022-198
Preprint. Discussion started: 6 May 2022

This paper has summarized improvements to the quality and accessibility of both coastal impact data products and related modeling platforms. The Sea Level Impacts Input Dataset by Elevation, Region and Scenarios (**SLIIDERS**) dataset represents a globally comprehensive and consistent collection of physical, ecological and socioeconomic variables for roughly ten thousand coastal localities. SLIIDERS is a segment-wise data product for coastal impacts, similar to previous products like DIVA (Vafeidis et al., 2008), but with significant improvements to the quality of represented variables and as an open-source resource following FAIR guidelines (Wilkinson et al., 2016). Any researcher can download, inspect and alter SLIIDERS to utilize in their own coastal modeling studies.

The Python-Coastal Impacts and Adaptation Model (pyCIAM), a companion model that utilizes SLIIDERS as an input, was developed as an open-source update to the original Coastal Impacts and Adaptation Model Diaz (2016) which incorporates numerous improvements to model functionality and efficiency. pyCIAM is also made available as a modular, open-source tool meant to be modified by users seeking to add functionality or improve input sources, with users able to combine the model with their own input datasets, provided they are formatted similarly to SLIIDERS. An additional key advance of pyCIAM is that it is designed to simulate impacts from tens to hundreds of thousands of future SLR scenarios in parallel, facilitating scalable probabilisitic impact modeling research.

Results from pyCIAM v1.0, paired with SLIIDERS v1.0, show the model produces roughly similar estimates of the net present cost of SLR-driven costs to those of CIAM (Diaz, 2016) under the SSP5 socioeconomic scenario, with all other SSP-IAM configurations producing smaller values (Fig. 5). Median annual, end of century costs under optimal adaptation in pyCIAM are also very similar to CIAM when averaging across all SSPs and growth models. When prohibiting proactive adaptation, costs are higher in pyCIAM for almost all scenarios as compared to CIAM. However, when comparing total yearly coastal damages, rather than just the climate-driven component, pyCIAM projects global NPV of all coastal damages between 2000-2100 to be roughly 3-4× those of CIAM (B1), likely due to greater population and capital stock estimates in these SSPs as compared to the trajectories used in Diaz (2016). The median annual, end of century total costs under optimal adaptation in pyCIAM are also higher than CIAM for all scenarios, with only the SSP4-IIASA scenario producing similar values.

Despite the improvements represented by the SLIIDERS data product and pyCIAM platform, there are aspects of them that should be improved in the future. We believe that a priority for future work should be to incorporate empirical evidence on coastal damages and adaptation behavior due to rising and extreme sea levels in order to better inform model assumptions. We hope that improvements to SLIIDERS can be made regularly as new, higher quality data sources for each of its constituent variables are mode available. Additionally, the segmentation of coastlines in SLIIDERS v1.0 can likely be improved beyond a uniform (50km) spacing nested at the country level to better delineate between coastal regions that are more likely to represent autonomous, decision making units, such as extents of coastal urban centers. We intend to make many of these improvements moving forward, and will make updated versions available as such efforts are carried out. However, our hope is that the open-source nature of both SLIIDERS and pyCIAM will enable community-driven development to spur more rapid and substantial improvements to both tools.

https://doi.org/10.5194/egusphere-2022-198
Preprint. Discussion started: 6 May 2022

5 Code and data availability

Version 1.0 of SLIIDERS, including both SLIIDERS-ECON and SLIIDERS-SLR, is associated with the results presented in this manuscript. The datasets are available at https://doi.org/10.5281/zenodo.6449231, and the associated pre-processing code is available at https://github.com/ClimateImpactLab/sliiders and additionally via Zenodo at https://doi.org/10.5281/zenodo.6456115. The outputs of the pyCIAM model, as presented in this manuscript, are hosted at https://doi.org/10.5281/zenodo.6014086. The pyCIAM model is available at https://github.com/ClimateImpactLab/pyCIAM, on PyPI as the *python-CIAM* package, and via Zenodo at https://doi.org/10.5281/zenodo.6453099. Scripts and notebooks associated with the creation of results contained in this manuscript are also included in the pyCIAM GitHub repository and Zenodo repository. For both the SLIIDERS and pyCIAM code repositories on GitHub and Zenodo, version 1.0.2 is the version associated with this manuscript.

Appendix A: Supplemental Information

A1 Coastlines Creation and Length Calculation

To create each segment represented in SLIIDERS and used in pyCIAM, we assembled a set of polylines according to the following steps[3]:

1. Downloaded 1:50m and 1:10m Natural Earth Coastlines (www.naturalearthdata.com/downloads/). For the majority of segments, the moderately resolved 1:50m coastlines were used, with the fine scale of the 1:10m layer required for small island polygons not represented in the 1:50m layer.
2. Removed Caspian Sea borders from both coastline layers to avoid modeling along this inland sea.
3. Removed all line segments south of 60S (Antarctica) from both coastline layers to avoid inclusion of these coastlines in any final coastal segments, due to the lack of population and capital exposure any latitudes below 60S.
4. Converted both coastline layers to polygons in order to get land areas that correspond to the fine (1:10m) and medium (1:50m) scale coastline resolutions.
5. identified all land area polygons derived from the 1:10m coastline layer that are not represented by 1:50m coastlines, which preserves many smaller island areas.
6. Merged these 1:10m polygons with the 1:50m polygons into a single layer
7. Intersected resulting polygon layer of land masses with exposure grid of population and capital assets, and removed land masses that contained no capital or population exposure. In these completely un-populated areas, we cannot accurately represent value of lost land within the pyCIAM framework, nor is this value likely to be large.
8. Converted this hybrid 1:10m and 1:50m land area polygon layer back to polylines for use as our final vector layer of global coastlines.

[3]Steps 2-6 and 8 used the Quantum Geographical Information Systems (QGIS) v3.16 software.

https://doi.org/10.5194/egusphere-2022-198
Preprint. Discussion started: 6 May 2022

9. Constructed a set of Voronoi polygons from the CoDEC-derived coastal segment centroids and intersected these with the coastlines layer constructed in Steps 1-8. This partitioned coastlines according to segment, allowing for the calculation of the total length (in kilometers) of coastline by coastal segment.

A2 Aligning geographic and socioeconomic datasets to build SLIIDERS-ECON

Socioeconomic variables expressed in SLIIDERS-ECON and used in pyCIAM are defined at various geographic aggregation levels, from the fine "elevation bin by admin-1 region" scale to the coarse country scale. Input data sources also come in various formats, from gridded estimates of coastal elevation, population and capital distribution, and wetland area, to country-level SSP-based projections of income, population, and capital growth trajectories, to vector representations of country boundaries and coastlines. To create SLIIDERS-ECON, we must harmonize these various input sources. We start by assigning admin-1 and country labels to each grid cell in the gridded elevation and exposure input sources, using boundaries from GADM v3.6. Notably, GADM considers as a "country" any region with an ISO country code, regardless of sovereignty.

There are 199 such countries that are coastal and contain non-zero land under 20 m elevation. The boundaries of the admin-1 regions within these 199 countries are overlaid on gridded elevation and exposure datasets, including those defining spatial distributions of population (LANDSCAN 2019) and physical capital (LitPop and GEG-15), to assign elevations and admin-1 labels to each grid cell. The gridded dryland and wetland area, population, and physical capital estimates are then binned by 10 cm elevation increments and grouped within admin-1 regions and coastal segments. Each admin-1 region is then assigned its corresponding country label, which is matched to the SSP-based country-level growth trajectories.

A3 Imputing initial-year (2010) capital stock values

Out of the 199 countries included in SLIIDERS-ECON, 146 have capital stock values in 2010 in PWT 10.0 that we use as initial conditions for projecting capital stock consistent with the SSPs. We must impute the 53 remaining values; while only 2010 values are needed to seed the capital growth model, we take an approach that allows for simultaneous estimation of a time series of capital stock beginning in 1950. This approach generates estimates of historical capital consistent with those of other ongoing work. Our estimation process consists of the following steps:

1. We impute any missing historical GDP estimates from 1950-2020 (Section A3.1) within our aggregation of GDP data sources (Sect. 2.6.2).
2. We estimate the relationship between historical investment-to-GDP ratio, income, and population share values, and impute historical investment, following Higgins (1998) (Section A3.2).
3. For the countries with 2005 capital stock estimates in GEG-15 (Bono and Chatenoux, 2014) and 2014 estimates in LitPop (Eberenz et al., 2020), but with no estimates in PWT 10.0, we exponentially interpolate to 2010.
4. For the remaining countries with 2005 estimates in GEG-15 but no 2014 estimates in LitPop, we use the perpetual inventory method with historical investment estimates from Step 2 to estimate 2010 capital stock.

https://doi.org/10.5194/egusphere-2022-198
Preprint. Discussion started: 6 May 2022

5. For the remaining countries with 2014 estimates in LitPop but no 2005 estimates in GEG-15 or PWT 10.0, we first estimate the 1950 capital stock values following Inklaar et al. (2019) using the actual and estimated GDP and investment-to-GDP ratio. Then, we exponentially interpolate to 2010.
6. For the final set of countries with no capital stock estimates in any of these three sources, we follow Eberenz et al. (2020) and estimate the 2014 capital stock values by multiplying GDP estimates by a capital-to-GDP ratio of 1.24724 from Credit Suisse Research Institute (2017). Then, we follow Step 5 to obtain 2010 estimates.

In the parts below, we describe the processes for imputing missing historical GDP and income values, historical investment-to-GDP ratios, and missing capital depreciation rates, and for estimating the missing 1950 capital stock values.

A3.1 Imputing missing historical (1950-2020) GDP

The capital stock imputation described above relies, in some cases, on a complete time series of GDP. While this exists for many countries after aggregating across the multiple data sources described in Sect. 2.6.2, some countries and territories are missing observations for some of this time series. For territories, whose growth often converges to that of the corresponding sovereign state (Bertram, 2004), we impute GDP in missing years using the average ratio of the territory's GDP to that of the sovereign state during non-missing years. For other cases, we find five "nearest" countries, such that the sum of squared differences of yearly GDP growth rates to that of the target country are minimized across all non-missing years. We then impute the growth rates for missing years using a weighted average of these five end members, weighted by the inverse of the SSEs, and interpolate/extrapolate around non-missing observation using these growth rates.

A3.2 Imputing missing historical (1950-2020) investment-to-GDP ratios

Investment-to-GDP ratios are imputed via a regression across non-missing years of this ratio on per capita GDP levels and growth rates as well as population age distributions. The regression used is borrowed from Foure et al. (2012) and adjusted R^2, AIC, and BIC are compared across models with and without the age distribution variables. The model that includes those variables performs better and thus we use that model for the necessary imputations. See the code repository that accompanies this manuscript for further details on method and for a summary of regression results.

A3.3 Imputing missing capital depreciation rates

We use PWT 10.0 as our main source for historical capital depreciation rates. However, many of the countries considered in our workflow are either not included in PWT 10.0, or they are included but are missing values for certain years. In these cases, we impute the depreciation rate of country j in year t by taking an unweighted average of the available depreciation rates across all countries in year t. To project future capital depreciation for each country, necessary to project future capital stock levels, we simply extend our estimates of 2010 capital depreciation rates to all future years. The projection method described in Dellink et al. (2017) also requires a global capital depreciation rate used when deriving long-run investment-to-GDP ratios,

https://doi.org/10.5194/egusphere-2022-198
Preprint. Discussion started: 6 May 2022

for which we use the 2010 global average depreciation rate in PWT 10.0, which is approximately 4.416%, comparable to the 5% global depreciation rate used in Dellink et al. (2017).

A3.4 Imputing 1950 capital stock

We follow the method used in PWT 10.0 (Inklaar et al., 2019) to estimate capital stock in 1950 where needed for imputation, using GDP and investment-to-GDP ratios estimated from the data sources compiled in Sect. 2.6.2 and imputed via the previously described approaches. We update the bounds and annual increment of capital intensity (a.k.a. capital-to-GDP ratio) used in the algorithm based on the compiled data. Inklaar et al. (2019) sets bounds of [0.5, 4.0] and an annual increment of 0.02; however, capital intensities and their increments vary greatly across countries. Thus, we apply a k-means clustering analysis of the 2014-2020 capital intensity values to classify countries into three groups based on their capital intensity values and growth rates. As a result, we use the following triples of lower bound, upper bound, and annual increment of capital intensity for each cluster: (0.861, 3.902, 0.014), (1.810, 6.298, 0.037), and (2.616, 13.853, 0.166). Note that as opposed to using minimum and maximum values as the lower and upper capital intensity bounds as in Inklaar et al. (2019), we use bottom and top decile within each cluster due to heavy tailed distributions of capital intensity in PWT 10.0.

A4 Projecting SSP-consistent (2010-2100) capital stock values

Using actual and imputed historical 2010 country-level capital stocks as initial conditions, we extract the capital portion of the OECD Env-Growth model (Dellink et al., 2017) and apply it to the SSP trajectories of GDP and population. The model requires global GDP elasticity of capital and 2010 country-level marginal products of capital (MPK), which are not described in Dellink et al. (2017). We use a global GDP elasticity of capital of 0.326 from Crespo Cuaresma (2017) and estimate 2010 MPKs using a modified Cobb-Douglas production function that contains only capital inputs. Coefficients of the function are derived by fitting to the compiled dataset of historical GDP and capital. Alternative approaches for obtaining these necessary inputs, including the use of a production function with labor and capital inputs and deriving the global elasticity directly from the production function, were also evaluated; however, these approaches yielded greater discrepancies in projected capital stocks when compared with the limited set of results presented in Dellink et al. (2017).

Appendix B: Supplemental Figures

https://doi.org/10.5194/egusphere-2022-198
Preprint. Discussion started: 6 May 2022

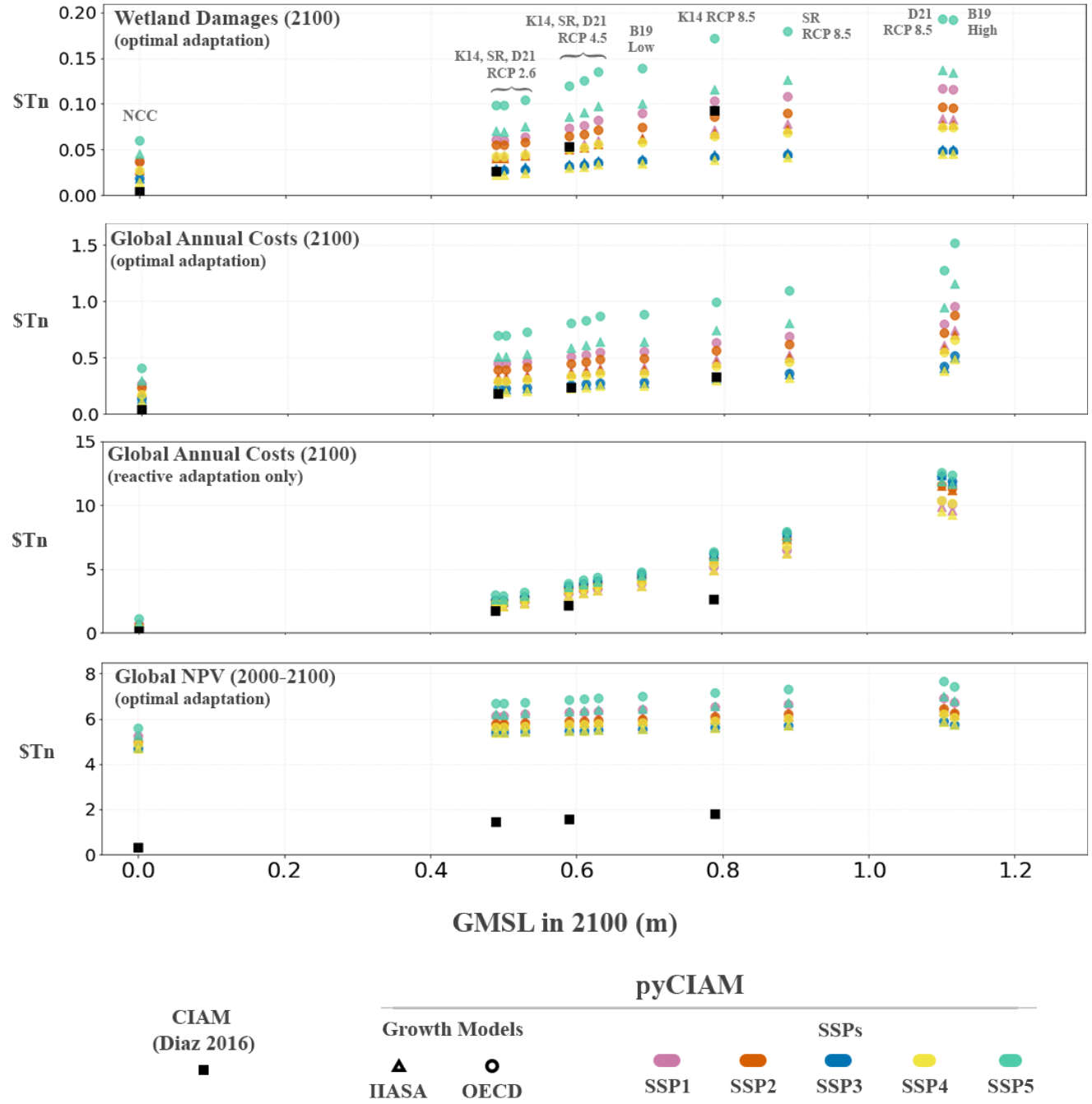

Figure B1. Comparison of four global cost metrics for median model results under each SLR scenario, for CIAM (black) and pyCIAM (colored). Values represent total coastal losses (inclusive of hazards not attributable to climate change). All costs are expressed in constant 2019 PPP USD. Each vertical group of points represents a single SLR scenario (Table 3), with each point in the group representing a unique combination of SSP and growth model. Differencing the values associated with 0 GMSL rise from the other values yields Fig. 5. n.b. The D21-RCP8.5 and B19-High SLR scenarios share the same projected GMSL in 2100 (1.11m) and were jittered by +/- 0.007m for plotting clarity.

https://doi.org/10.5194/egusphere-2022-198
Preprint. Discussion started: 6 May 2022

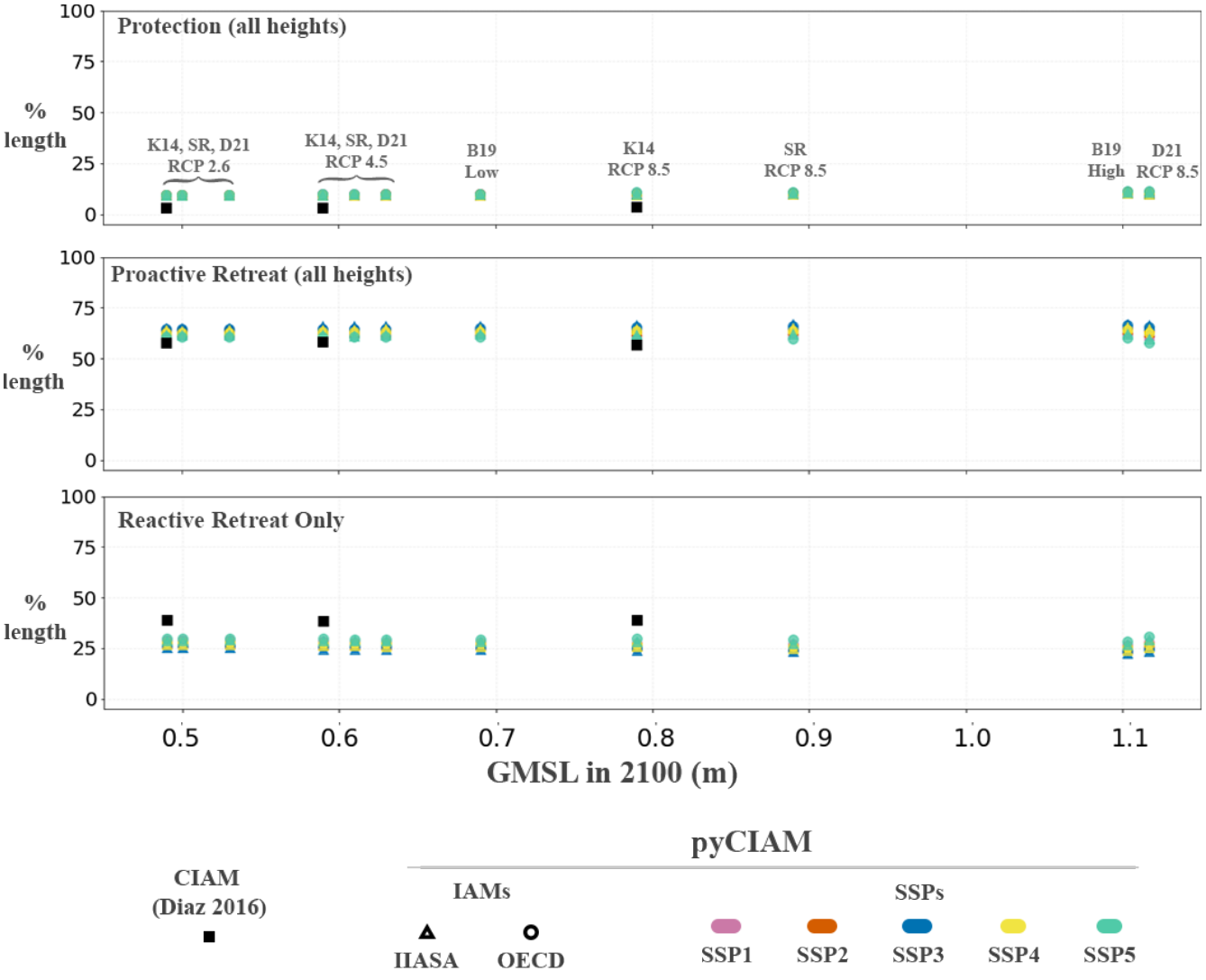

Figure B2. Comparison of optimal adaptation strategies adopted across all segments. Values represent percentages of global coastline associated with segments adopting each respective adaptation strategy. Proactive retreat and protection values are aggregates of all possible heights for each. Solid black squares represent the results from Diaz (2016) and the colored circle and triangle markers represent pyCIAM/SLIIDERS results for all SLR (differentiated by GMSL values), SSP and growth model scenarios. n.b. The D21-RCP8.5 and B19-High SLR scenarios share the same projected GMSL in 2100 (1.11m) and were jittered by +/- 0.007m for plotting clarity.

https://doi.org/10.5194/egusphere-2022-198
Preprint. Discussion started: 6 May 2022

Appendix C: Supplemental Tables

https://doi.org/10.5194/egusphere-2022-198
Preprint. Discussion started: 6 May 2022

Input Dataset	Source & Description	DOI
Coastal Segments	**CoDEC, Natural Earth** (Muis et al., 2020) Thinned European coastal points in CoDEC from 10km spacing to 50km and made 15 manual additions to ensure all countries contain at least one segment. Coastline shapes were taken from Natural Earth (1:50m and 1:10m).	10.5281/zenodo.3660927 (Unaltered CoDEC)
Extreme sea levels (ESLs)	**CoDEC** (Muis et al., 2020) ESL values in CoDEC are calculated from the Global Tide and Surge Model (GTSMv3.0)	10.5281/zenodo.3660927 (Unaltered CoDEC)
Elevation	**CoastalDEM v1.1** (Kulp and Strauss, 2019) Corrects significant high bias of coastal elevations found in previous DEMs (e.g. SRTM) **SRTM15+ v2.3** (Tozer et al., 2019) Global topography and bathymetry at 15 arc-second resolution. Used wherever CoastalDEM is undefined **MDT Global CNES-CLS18** (Mulet et al., 2021) Mean dynamic topography at $1/8°$ resolution **XGM2019e** (Zingerle et al., 2020) Experimental gravity field model at 2 arc-minute resolution	10.1038/s41467-019-12808-z 10.1029/2019EA000658 10.5194/os-17-789-2021 10.1007/s00190-020-01398-0
Wetland and Mangrove Extent	**GLOBCOVER v2.3** (European Space Agency and UCLouvain, 2010) (wetlands) **Global Mangrove Watch 2016** (Bunting et al., 2018) (mangroves)	N/A 10.3390/rs1010669
Sea level rise projections	**LocalizeSL** (projections corresponding to Kopp et al., 2014; Bamber et al., 2019; Oppenheimer et al., 2019; DeConto et al., 2021)] Localized probabilistic estimates of global SLR at each coastal segment conditional on a certain level of global SLR in a certain year and under a variety of physical assumptions	10.5281/zenodo.6029807

Table C1. Summary of SLIIDERS datasets and pyCIAM inputs for physical variables.

https://doi.org/10.5194/egusphere-2022-198
Preprint. Discussion started: 6 May 2022

Input Dataset	Source & Description
Current Population	**LandScan 2019** (Rose et al., 2020) Spatial distribution of global population in 2019 at a 30 arc-second resolution (∼1km at equator) **PWT 10.0** (Feenstra et al., 2015), **UN World Population Prospects** (UN DESA, 2019) Country-level population estimates
Current Income	**PWT 10.0** (Feenstra et al., 2015) **World Bank World Development Indicators** (Bank, 2021) **IMF World Economic Outlook** (IMF, 2021) **Maddison Project Database** (Bolt and van Zanden, 2020) **OECD regional statistics** (for Economic Cooperation and Development, 2020) **CIA World Factbook** (Agency, 2021) Collection of contemporary datasets to estimate national income levels
Physical capital	**LitPop** (Eberenz et al., 2020), **2015 Global Assessment Report (GEG-15)** (Bono and Chatenoux, 2014) Spatially downscaled (30 arc-second and $1/24°$, respectively) estimates of physical capital stock **PWT 10.0** (Feenstra et al., 2015) Country-level physical capital stock levels
Mobile capital fraction	**PWT 10.0** (Feenstra et al., 2015) Capital is reported in PWT by category; structures are assumed to be immobile, with all other categories assumed as mobile
Economic growth trajectories	**Shared Socioeconomic Pathways** (Riahi et al., 2017) and capital growth modeled by **Dellink et al. 2017** (Dellink et al., 2017) Updated growth trajectories to match those used by the IPCC
Construction cost indices	**World Bank ICP** (World Bank, 2020; Lincke and Hinkel, 2021)

Table C2. Summary of SLIIDERS datasets and pyCIAM inputs for socioeconomic variables.

https://doi.org/10.5194/egusphere-2022-198
Preprint. Discussion started: 6 May 2022

Author contributions. Project conceptualized by IB, SH, REK. Data curation by DA, IB, JC, ND, AH. Methodology development, investigation, and formal analysis conducted by DA, IB, JC, ND. Map and figure visualizations were done by ND. Code base developed by DA, IB, JC, ND. Software developed by DA, IB, JC and ND. Model validation performed by IB and ND. Project administered by IB, ND, SH. Original draft written by IB, JC, DA, ND. Manuscript review and editing by DA, IB, JC, ND, SH, REK, MG. Funding acquisition by MG, SH, TH, REK. Supervision by MD, MG, SH, REK.

Competing interests. The authors declare that they have no conflict of interest

Acknowledgements. We thank Maya Norman for conducting her review and evaluation of relevant exposure datasets. Thank you also to Delavane Diaz, who contributed invaluable assistance in the access and interpretation of the CIAM model. We also thank members of the Climate Impact Lab who provided important feedback and guidance during frequent discussions about model objectives and developments. This project is an output of the Climate Impact Lab that gratefully acknowledges funding from the Energy Policy Institute of Chicago (EPIC), International Growth Centre, National Science Foundation (ICER-1663807), Sloan Foundation, Carnegie Corporation, and Tata Center for Development.

https://doi.org/10.5194/egusphere-2022-198
Preprint. Discussion started: 6 May 2022

References

Global Land One-kilometer Base Elevation (GLOBE), Documentation, National Oceanic and Atmospheric Administration, Boulder, CO, https://www.ngdc.noaa.gov/mgg/topo/report/globedocumentationmanual.pdf, 1999.

Agency, C. I.: The World Factbook, https://www.cia.gov/the-world-factbook/, 2021.

Armstrong, S. B., Lazarus, E. D., Limber, P. W., Goldstein, E. B., Thorpe, C., and Ballinger, R. C.: Indications of a positive feedback between coastal development and beach nourishment, Earth's Future, 4, 626–635, https://doi.org/10.1002/2016EF000425, 2016.

Bakkensen, L. A. and Mendelsohn, R. O.: Risk and Adaptation: Evidence from Global Hurricane Damages and Fatalities, Journal of the Association of Environmental and Resource Economists, 3, 555–587, https://doi.org/10.1086/685908, 2016.

Bakkensen, L. A., Park, D.-S. R., and Sarkar, R. S. R.: Climate costs of tropical cyclone losses also depend on rain, Environmental Research Letters, 13, 074 034, https://doi.org/10.1088/1748-9326/aad056, 2018.

Bamber, J. L., Oppenheimer, M., Kopp, R. E., Aspinall, W. P., and Cooke, R. M.: Ice sheet contributions to future sea-level rise from structured expert judgment, Proceedings of the National Academy of Sciences, 116, 11 195–11 200, https://doi.org/10.1073/pnas.1817205116, 2019.

Bank, T. W.: World Development Indicators, https://datacatalog.worldbank.org/dataset/world-development-indicators, 2021.

Berrang-Ford, L., Siders, A. R., Lesnikowski, A., Fischer, A. P., Callaghan, M. W., Haddaway, N. R., Mach, K. J., Araos, M., Shah, M. A. R., Wannewitz, M., Doshi, D., Leiter, T., Matavel, C., Musah-Surugu, J. I., Wong-Parodi, G., Antwi-Agyei, P., Ajibade, I., Chauhan, N., Kakenmaster, W., Grady, C., Chalastani, V. I., Jagannathan, K., Galappaththi, E. K., Sitati, A., Scarpa, G., Totin, E., Davis, K., Hamilton, N. C., Kirchhoff, C. J., Kumar, P., Pentz, B., Simpson, N. P., Theokritoff, E., Deryng, D., Reckien, D., Zavaleta-Cortijo, C., Ulibarri, N., Segnon, A. C., Khavhagali, V., Shang, Y., Zvobgo, L., Zommers, Z., Xu, J., Williams, P. A., Canosa, I. V., van Maanen, N., van Bavel, B., van Aalst, M., Turek-Hankins, L. L., Trivedi, H., Trisos, C. H., Thomas, A., Thakur, S., Templeman, S., Stringer, L. C., Sotnik, G., Sjostrom, K. D., Singh, C., Siña, M. Z., Shukla, R., Sardans, J., Salubi, E. A., Safaee Chalkasra, L. S., Ruiz-Díaz, R., Richards, C., Pokharel, P., Petzold, J., Penuelas, J., Pelaez Avila, J., Murillo, J. B. P., Ouni, S., Niemann, J., Nielsen, M., New, M., Nayna Schwerdtle, P., Nagle Alverio, G., Mullin, C. A., Mullenite, J., Mosurska, A., Morecroft, M. D., Minx, J. C., Maskell, G., Nunbogu, A. M., Magnan, A. K., Lwasa, S., Lukas-Sithole, M., Lissner, T., Lilford, O., Koller, S. F., Jurjonas, M., Joe, E. T., Huynh, L. T. M., Hill, A., Hernandez, R. R., Hegde, G., Hawxwell, T., Harper, S., Harden, A., Haasnoot, M., Gilmore, E. A., Gichuki, L., Gatt, A., Garschagen, M., Ford, J. D., Forbes, A., Farrell, A. D., Enquist, C. A. F., Elliott, S., Duncan, E., Coughlan de Perez, E., Coggins, S., Chen, T., Campbell, D., Browne, K. E., Bowen, K. J., Biesbroek, R., Bhatt, I. D., Bezner Kerr, R., Barr, S. L., Baker, E., Austin, S. E., Arotoma-Rojas, I., Anderson, C., Ajaz, W., Agrawal, T., and Abu, T. Z.: A systematic global stocktake of evidence on human adaptation to climate change, Nature Climate Change, 11, 989–1000, https://doi.org/10.1038/s41558-021-01170-y, 2021.

Bertram, G.: On the Convergence of Small Island Economies with Their Metropolitan Patrons, World Development, 32, 343–364, https://doi.org/10.1016/j.worlddev.2003.08.004, 2004.

Bolt, J. and van Zanden, J. L.: Maddison style estimates of the evolution of the world economy. A new 2020 update, Maddison-Project Working Paper, pp. 1–43, https://www.rug.nl/ggdc/historicaldevelopment/maddison/publications/wp15.pdf, 2020.

Bono, A. D. and Chatenoux, B.: A Global Exposure Model for GAR 2015, Input Paper prepared for the Global Assessment Report on Disaster Risk Reduction, The United Nations Office for Disaster Risk Reduction, Geneva, Switzerland, https://www.preventionweb.net/english/hyogo/gar/2015/en/bgdocs/risk-section/De%20Bono,%20Andrea,%20Bruno%20Chatenoux.%202015.%20A%20Global%20Exposure%20Model%20for%20GAR%202015,%20%20UNEP-GRID.pdf, 2014.

https://doi.org/10.5194/egusphere-2022-198
Preprint. Discussion started: 6 May 2022

Bower, E. and Weerasinghe, S.: Enhancing the Evidence Base on Planned Relocation Cases in the Context of Hazards, Disasters, and Climate Change, 2021.

Bunting, P., Rosenqvist, A., Lucas, R. M., Rebelo, L.-M., Hilarides, L., Thomas, N., Hardy, A., Itoh, T., Shimada, M., and Finlayson, C. M.: The Global Mangrove Watch—A New 2010 Global Baseline of Mangrove Extent, Remote Sensing, 10, 1669, https://doi.org/10.3390/rs10101669, 2018.

Carleton, T. A., Jina, A., Delgado, M. T., and Others: VALUING THE GLOBAL MORTALITY CONSEQUENCES OF CLIMATE CHANGE ACCOUNTING FOR ADAPTATION COSTS AND BENEFITS, NBER WORKING PAPER SERIES, 2020.

Council, M. M.: Natural Hazard Mitigation Saves: 2017 Interim Report, p. 22, 2017.

Craig, R. K.: Coastal adaptation, government-subsidized insurance, and perverse incentives to stay, Climatic Change, 152, 215–226, https://doi.org/10.1007/s10584-018-2203-5, 2019.

Credit Suisse Research Institute: Global Wealth Report 2017: Where Are We Ten Years after the Crisis?, Tech. rep., https://www.credit-suisse.com/about-us-news/en/articles/news-and-expertise/global-wealth-report-2017-201711.html, 2017.

Crespo Cuaresma, J.: Income projections for climate change research: A framework based on human capital dynamics, Global Environmental Change, 42, 226–236, https://doi.org/10.1016/j.gloenvcha.2015.02.012, 2017.

DeConto, R. M., Pollard, D., Alley, R. B., Velicogna, I., Gasson, E., Gomez, N., Sadai, S., Condron, A., Gilford, D. M., Ashe, E. L., Kopp, R. E., Li, D., and Dutton, A.: The Paris Climate Agreement and future sea-level rise from Antarctica, Nature, 593, 83–89, https://doi.org/10.1038/s41586-021-03427-0, 2021.

Dellink, R., Chateau, J., Lanzi, E., and Magné, B.: Long-term economic growth projections in the Shared Socioeconomic Pathways, Global Environmental Change, 42, 200–214, https://doi.org/10.1016/j.gloenvcha.2015.06.004, 2017.

Diaz, D. B.: Estimating global damages from sea level rise with the Coastal Impact and Adaptation Model (CIAM), Climatic Change, 137, 143–156, https://doi.org/10.1007/s10584-016-1675-4, 2016.

Dronkers, J., Gilbert, J. T. E., Butler, L. W., Carey, J. J., Campbell, J., James, E., Mckenzie, C., Misdorp, R., Quin, N., Vallianos, L., and Dadelszen, J. V.: Strategies for Adaptation to Sea Level Rise, 1990.

Eberenz, S., Stocker, D., Röösli, T., and Bresch, D. N.: Asset exposure data for global physical risk assessment, Earth System Science Data, 12, 817–833, https://doi.org/10.5194/essd-12-817-2020, 2020.

European Space Agency and UCLouvain: Globcover 2009, http://due.esrin.esa.int/page_globcover.php, 2010.

Feenstra, R. C., Inklaar, R., and Timmer, M. P.: The Next Generation of the Penn World Table, American Economic Review, 105, 3150–3182, https://doi.org/10.1257/aer.20130954, 2015.

for Economic Cooperation and Development, O.: Regions and Cities: OECD Statistics, https://stats.oecd.org/, 2020.

Foure, J., Bénassy-Quéré, A., and Fontagne, L.: The Great Shift: Macroeconomic Projections for the World Economy at the 2050 Horizon, SSRN Scholarly Paper ID 2004332, Social Science Research Network, Rochester, NY, https://doi.org/10.2139/ssrn.2004332, 2012.

Fox-Kemper, B., Hewitt, H. T., Xiao, C., Aðalgeirsdóttir, G., Drijfhout, S. S., Edwards, T. L., Golledge, N. R., Hemer, M., Kopp, R. E., and Krinner, G.: Ocean, cryosphere and sea level change, Climate change, 2021.

Gregory, J. M., Griffies, S. M., Hughes, C. W., Lowe, J. A., Church, J. A., Fukimori, I., Gomez, N., Kopp, R. E., Landerer, F., Cozannet, G. L., Ponte, R. M., Stammer, D., Tamisiea, M. E., and van de Wal, R. S. W.: Concepts and Terminology for Sea Level: Mean, Variability and Change, Both Local and Global, Surveys in Geophysics, 40, 1251–1289, https://doi.org/10.1007/s10712-019-09525-z, 2019.

Haasnoot, M., Brown, S., Scussolini, P., Jimenez, J. A., Vafeidis, A. T., and Nicholls, R. J.: Generic adaptation pathways for coastal archetypes under uncertain sea-level rise, Environmental Research Communications, 1, https://doi.org/10.1088/2515-7620/ab1871, 2019.

https://doi.org/10.5194/egusphere-2022-198
Preprint. Discussion started: 6 May 2022

Haer, T., Botzen, W. J., de Moel, H., and Aerts, J. C.: Integrating Household Risk Mitigation Behavior in Flood Risk Analysis: An Agent-Based Model Approach, Risk Analysis, 37, 1977–1992, https://doi.org/10.1111/risa.12740, 2017.

Hallegatte, S., Green, C., Nicholls, R. J., and Corfee-Morlot, J.: Future flood losses in major coastal cities, Nature Climate Change, 3, 802–806, https://doi.org/10.1038/nclimate1979, 2013.

Heston, A., Summers, R., and Aten, B.: Penn World Table Version 7.0, Tech. rep., Center for International Comparisons of Production, Income and Prices at the University of Pennsylvania, https://www.rug.nl/ggdc/productivity/pwt/pwt-releases/pwt-7.0, 2011.

Higgins, M.: Demography, National Savings, and International Capital Flows, International Economic Review, 39, 343–369, https://doi.org/10.2307/2527297, 1998.

Hinkel, J. and Klein, R. J. T.: Integrating knowledge to assess coastal vulnerability to sea-level rise: The development of the DIVA tool, Global Environmental Change, 19, 384–395, https://doi.org/10.1016/j.gloenvcha.2009.03.002, 2009.

Hinkel, J., van Vuuren, D. P., Nicholls, R. J., and Klein, R. J. T.: The effects of adaptation and mitigation on coastal flood impacts during the 21st century. An application of the DIVA and IMAGE models, Climatic Change, 117, 783–794, https://doi.org/10.1007/s10584-012-0564-8, 2013.

Hinkel, J., Lincke, D., Vafeidis, A. T., Perrette, M., Nicholls, R. J., Tol, R. S., Marzeion, B., Fettweis, X., Ionescu, C., and Levermann, A.: Coastal flood damage and adaptation costs under 21st century sea-level rise, Proceedings of the National Academy of Sciences of the United States of America, 111, 3292–3297, https://doi.org/10.1073/pnas.1222469111, 2014.

Hinkel, J., Aerts, J. C. J. H., Brown, S., Jiménez, J. A., Lincke, D., Nicholls, R. J., Scussolini, P., Sanchez-Arcilla, A., Vafeidis, A., and Addo, K. A.: The ability of societies to adapt to twenty-first-century sea-level rise, Nature Climate Change, 8, 570–578, https://doi.org/10.1038/s41558-018-0176-z, 2018.

Hoozemans, F. M., Marchand, M., and Pennekamp, H.: A global vulnerability analysis: vulnerability assessment for population, coastal wetlands and rice production on a global scale, Technical Report 2nd Edition, Delft Hydraulics, The Netherlands, https://www.researchgate.net/publication/282669649_A_global_vulnerability_analysis_vulnerability_assessment_for_population_coastal_wetlands_and_rice_production_on_a_global_scale, 1993.

Houser, T., Hsiang, S., Kopp, R., Larsen, K., Delgado, M., Jina, A., Mastrandrea, M., Mohan, S., Muir-Wood, R., Rasmussen, D. J., Rising, J., and Wilson, P.: Economic Risks of Climate Change: An American Prospectus, Columbia University Press, 2015.

Hu, S., Niu, Z., and Chen, Y.: Global Wetland Datasets: a Review, Wetlands, 37, 807–817, https://doi.org/10.1007/s13157-017-0927-z, 2017.

IMF, I. M.: World Economic Outlook Database 2011, Tech. rep., https://www.imf.org/en/Publications/WEO/weo-database/2011/September, 2011.

IMF, I. M.: World Economic Outlook Database, April 2021, https://www.imf.org/en/Publications/WEO/weo-database/2021/April, 2021.

Inklaar, R., Woltjer, P., and Albarrán, D. G.: The Composition of Capital and Cross-Country Productivity Comparisons, International Productivity Monitor, 36, 34–52, https://ideas.repec.org/a/sls/ipmsls/v36y20192.html, 2019.

Jones, B. and O'Neill, B. C.: Spatially explicit global population scenarios consistent with the Shared Socioeconomic Pathways, Environmental Research Letters, 11, 084 003, https://doi.org/10.1088/1748-9326/11/8/084003, 2016.

Jonkman, S. and Vrijling, J.: Loss of life due to floods, Journal of Flood Risk Management, 1, 43–56, https://doi.org/10.1111/j.1753-318X.2008.00006.x, 2008.

Kopp, R. E., Horton, R. M., Little, C. M., Mitrovica, J. X., Oppenheimer, M., Rasmussen, D. J., Strauss, B. H., and Tebaldi, C.: Probabilistic 21st and 22nd century sea-level projections at a global network of tide-gauge sites, Earth's Future, 2, 383–406, https://doi.org/10.1002/2014ef000239, 2014.

https://doi.org/10.5194/egusphere-2022-198
Preprint. Discussion started: 6 May 2022

Kopp, R. E., DeConto, R. M., Bader, D. A., Hay, C. C., Horton, R. M., Kulp, S., Oppenheimer, M., Pollard, D., and Strauss, B. H.: Evolving Understanding of Antarctic Ice-Sheet Physics and Ambiguity in Probabilistic Sea-Level Projections, Earth's Future, 5, 1217–1233, https://doi.org/10.1002/2017EF000663, 2017.

Kopp, R. E., Gilmore, E. A., Little, C. M., Lorenzo-Trueba, J., Ramenzoni, V. C., and Sweet, W. V.: Usable Science for Managing the Risks of Sea-Level Rise, Earth's Future, 7, 1235–1269, https://doi.org/10.1029/2018EF001145, 2019.

Kulp, S. A. and Strauss, B. H.: CoastalDEM: A global coastal digital elevation model improved from SRTM using a neural network, Remote Sensing of Environment, 206, 231–239, https://doi.org/10.1016/j.rse.2017.12.026, 2018.

Kulp, S. A. and Strauss, B. H.: New elevation data triple estimates of global vulnerability to sea-level rise and coastal flooding, Nature Communications, 10, https://doi.org/10.1038/s41467-019-12808-z, 2019.

Lagerlöf, N.-P. and Basher, S. A.: Geography, population density, and per-capita income gaps across US states and Canadian provinces, 2005.

Lickley, M. J., Lin, N., and Jacoby, H. D.: Analysis of coastal protection under rising flood risk, Climate Risk Management, 6, 18–26, https://doi.org/10.1016/j.crm.2015.01.001, 2014.

Lincke, D. and Hinkel, J.: Economically robust protection against 21st century sea-level rise, Global Environmental Change, 51, 67–73, https://doi.org/10.1016/j.gloenvcha.2018.05.003, 2018.

Lincke, D. and Hinkel, J.: Coastal Migration due to 21st Century Sea-Level Rise, Earth's Future, 9, e2020EF001 965, https://doi.org/10.1029/2020EF001965, 2021.

Lorie, M., Neumann, J. E., Sarofim, M. C., Jones, R., Horton, R. M., Kopp, R. E., Fant, C., Wobus, C., Martinich, J., O'Grady, M., and Gentile, L. E.: Modeling coastal flood risk and adaptation response under future climate conditions, Climate Risk Management, 29, 100 233, https://doi.org/10.1016/j.crm.2020.100233, 2020.

McNamara, D. E. and Keeler, A.: A coupled physical and economic model of the response of coastal real estate to climate risk, Nature Climate Change, 3, 559–562, https://doi.org/10.1038/nclimate1826, 2013.

McNamara, D. E., Gopalakrishnan, S., Smith, M. D., and Murray, A. B.: Climate adaptation and policy-induced inflation of coastal property value, PLoS ONE, 10, 1–12, https://doi.org/10.1371/journal.pone.0121278, 2015.

Mendelsohn, R. O., Schiavo, J. G., and Felson, A.: Are American Coasts Under-Protected?, Coastal Management, 48, 23–37, https://doi.org/10.1080/08920753.2020.1691482, 2020.

Muis, S., Verlaan, M., Winsemius, H. C., Aerts, J. C. J. H., and Ward, P. J.: A global reanalysis of storm surges and extreme sea levels, Nature Communications, 7, 11 969, https://doi.org/10.1038/ncomms11969, 2016.

Muis, S., Apecechea, M. I., Dullaart, J., de Lima Rego, J., Madsen, K. S., Su, J., Yan, K., and Verlaan, M.: A High-Resolution Global Dataset of Extreme Sea Levels, Tides, and Storm Surges, Including Future Projections, Frontiers in Marine Science, 7, 263, https://doi.org/10.3389/fmars.2020.00263, 2020.

Mulet, S., Rio, M.-H., Etienne, H., Artana, C., Cancet, M., Dibarboure, G., Feng, H., Husson, R., Picot, N., Provost, C., and Strub, P. T.: The new CNES-CLS18 global mean dynamic topography, Ocean Science, 17, 789–808, https://doi.org/10.5194/os-17-789-2021, 2021.

Neumann, B., Vafeidis, A. T., Zimmermann, J., and Nicholls, R. J.: Future coastal population growth and exposure to sea-level rise and coastal flooding - A global assessment, PLoS ONE, 10, https://doi.org/10.1371/journal.pone.0118571, 2015.

Nicholls, R., Klein, R., and Tol, R.: Managing coastal vulnerability and climate change: a national to global perspective, 2006.

Nicholls, R. J.: Analysis of global impacts of sea-level rise: a case study of flooding, Physics and Chemistry of the Earth, Parts A/B/C, 27, 1455–1466, https://doi.org/10.1016/S1474-7065(02)00090-6, 2002.

https://doi.org/10.5194/egusphere-2022-198
Preprint. Discussion started: 6 May 2022

Nicholls, R. J.: Coastal flooding and wetland loss in the 21st century: changes under the SRES climate and socio-economic scenarios, Global Environmental Change, 14, 69–86, https://doi.org/10.1016/j.gloenvcha.2003.10.007, 2004.

O'Neill, B. C., Kriegler, E., Ebi, K. L., Kemp-Benedict, E., Riahi, K., Rothman, D. S., van Ruijven, B. J., van Vuuren, D. P., Birkmann, J., Kok, K., Levy, M., and Solecki, W.: The roads ahead: Narratives for shared socioeconomic pathways describing world futures in the 21st century, Global Environmental Change, 42, 169–180, https://doi.org/10.1016/j.gloenvcha.2015.01.004, 2017.

Oppenheimer, M., Glavovic, B., Hinkel, J., van de Wal, R., Magnan, A. K., Abd-Elgawad, A., Cai, R., Cifuentes-Jara, M., Deconto, R. M., Ghosh, T., Hay, J., Isla, F., Marzeion, B., Meyssignac, B., and Sebesvari, Z.: Chapter 4: Sea Level Rise and Implications for Low Lying Islands, Coasts and Communities, in: IPCC Special Report on the Ocean and Cryosphere in a Changing Climate, edited by P\"ortner, H.-O., Roberts, D. C., Masson-Delmotte, V., Zhai, P., Tignor, M., Poloczanska, E., Mintenbeck, K., Alegr\'eia, A., Nicolai, M., Okem, A., Petzold, J., Rama, B., and Weyer, N. M., 2019.

Pardaens, A. K., Lowe, J. A., Brown, S., Nicholls, R. J., and de Gusmão, D.: Sea-level rise and impacts projections under a future scenario with large greenhouse gas emission reductions, Geophysical Research Letters, 38, https://doi.org/10.1029/2011GL047678, 2011.

Rasmussen, D. J., Buchanan, M. K., Kopp, R. E., and Oppenheimer, M.: A Flood Damage Allowance Framework for Coastal Protection With Deep Uncertainty in Sea Level Rise, Earth's Future, 8, e2019EF001 340, https://doi.org/10.1029/2019EF001340, 2020.

Riahi, K., van Vuuren, D. P., Kriegler, E., Edmonds, J., O'Neill, B. C., Fujimori, S., Bauer, N., Calvin, K., Dellink, R., Fricko, O., Lutz, W., Popp, A., Cuaresma, J. C., Kc, S., Leimbach, M., Jiang, L., Kram, T., Rao, S., Emmerling, J., Ebi, K., Hasegawa, T., Havlik, P., Humpenöder, F., Da Silva, L. A., Smith, S., Stehfest, E., Bosetti, V., Eom, J., Gernaat, D., Masui, T., Rogelj, J., Strefler, J., Drouet, L., Krey, V., Luderer, G., Harmsen, M., Takahashi, K., Baumstark, L., Doelman, J. C., Kainuma, M., Klimont, Z., Marangoni, G., Lotze-Campen, H., Obersteiner, M., Tabeau, A., and Tavoni, M.: The Shared Socioeconomic Pathways and their energy, land use, and greenhouse gas emissions implications: An overview, Global Environmental Change, 42, 153–168, https://doi.org/10.1016/j.gloenvcha.2016.05.009, 2017.

Rode, A., Carleton, T., Delgado, M., Greenstone, M., Houser, T., Hsiang, S., Hultgren, A., Jina, A., Kopp, R. E., McCusker, K. E., Nath, I., Rising, J., and Yuan, J.: Estimating a social cost of carbon for global energy consumption, Nature, 598, 308–314, https://doi.org/10.1038/s41586-021-03883-8, 2021.

Rodriguez, E., Morris, C. S., Belz, J. E., Chapin, E. C., Martin, J. M., Daffer, W., and Hensley, S.: An assessment of the SRTM topographic products, 2005.

Román, M. O., Wang, Z., Sun, Q., Kalb, V., Miller, S. D., Molthan, A., Schultz, L., Bell, J., Stokes, E. C., Pandey, B., Seto, K. C., Hall, D., Oda, T., Wolfe, R. E., Lin, G., Golpayegani, N., Devadiga, S., Davidson, C., Sarkar, S., Praderas, C., Schmaltz, J., Boller, R., Stevens, J., Ramos González, O. M., Padilla, E., Alonso, J., Detrés, Y., Armstrong, R., Miranda, I., Conte, Y., Marrero, N., MacManus, K., Esch, T., and Masuoka, E. J.: NASA's Black Marble nighttime lights product suite, Remote Sensing of Environment, 210, 113–143, https://doi.org/10.1016/j.rse.2018.03.017, 2018.

Rose, A. N., McKee, J. J., Sims, K. M., Bright, E. A., Reith, A. E., and Urban, M. L.: LandScan 2019, https://landscan.ornl.gov/, 2020.

Sadoff, C. W., Hall, J. W., Grey, D., Aerts, J. C. J. H., Ait-Kadi, M., Brown, C., Cox, A., Dadson, S., Garrick, D., Kelman, J., McCornick, P., Ringler, C., Rosegrant, M., Whittington, D., and Wiberg, D.: Securing water, sustaining growth. Report of the GWP/OECD Task Force on Water Security and Sustainable Growth, Tech. rep., University of Oxford, http://www.water.ox.ac.uk/wp-content/uploads/2015/04/SCHOOL-OF-GEOGRAPHY-SECURING-WATER-SUSTAINING-GROWTH-DOWNLOADABLE.pdf, 2015.

https://doi.org/10.5194/egusphere-2022-198
Preprint. Discussion started: 6 May 2022

Scussolini, P., Aerts, J. C. J. H., Jongman, B., Bouwer, L. M., Winsemius, H. C., de Moel, H., and Ward, P. J.: FLOPROS: an evolving global database of flood protection standards, Natural Hazards and Earth System Sciences, 16, 1049–1061, https://doi.org/10.5194/nhess-16-1049-2016, 2016.

Suckall, N., Tompkins, E. L., Nicholls, R. J., Kebede, A. S., Lázár, A. N., Hutton, C., Vincent, K., Allan, A., Chapman, A., Rahman, R., Ghosh, T., and Mensah, A.: A framework for identifying and selecting long term adaptation policy directions for deltas, Science of the Total Environment, 633, 946–957, https://doi.org/10.1016/j.scitotenv.2018.03.234, 2018.

Sweet, W., Horton, R., Kopp, R., LeGrande, A., and Romanou, A.: Ch. 12: Sea Level Rise. Climate Science Special Report: Fourth National Climate Assessment, Volume I, Tech. rep., U.S. Global Change Research Program, https://doi.org/10.7930/J0VM49F2, 2017.

Taylor, K. E., Stouffer, R. J., and Meehl, G. A.: An Overview of CMIP5 and the Experiment Design, Bulletin of the American Meteorological Society, 93, 485–498, https://doi.org/10.1175/BAMS-D-11-00094.1, 2012.

Tiggeloven, T., Moel, H. d., Winsemius, H. C., Eilander, D., Erkens, G., Gebremedhin, E., Loaiza, A. D., Kuzma, S., Luo, T., Iceland, C., Bouwman, A., Huijstee, J. v., Ligtvoet, W., and Ward, P. J.: Global-scale benefit-cost analysis of coastal flood adaptation to different flood risk drivers using structural measures., Natural Hazards and Earth System Sciences, 20, 1025–1025, https://go.gale.com/ps/i.do?p=AONE&sw=w&issn=15618633&v=2.1&it=r&id=GALE%7CA621126931&sid=googleScholar&linkaccess=fulltext, 2020.

Tol, R. S. J.: The damage costs of climate change towards a dynamic representation, Ecological Economics, 19, 67–90, https://doi.org/10.1016/0921-8009(96)00041-9, 1996.

Tozer, B., Sandwell, D. T., Smith, W. H. F., Olson, C., Beale, J. R., and Wessel, P.: Global Bathymetry and Topography at 15 Arc Sec: SRTM15+, Earth and Space Science, 6, 1–18, https://doi.org/10.1029/2019EA000658, 2019.

UN DESA, Department of Economic and Social Affairs, P. U. N.: World Population Prospects 2012: Volume I: Comprehensive Tables, Tech. rep., https://population.un.org/wpp/Publications/Files/WPP2019_Volume-I_Comprehensive-Tables.pdf, 2012.

UN DESA, Department of Economic and Social Affairs, P. U. N.: World Population Prospects 2019: Volume I: Comprehensive Tables, Tech. rep., https://population.un.org/wpp/Publications/Files/WPP2019_Volume-I_Comprehensive-Tables.pdf, 2019.

University, C. F. I. E. S. I. N.-C.-C.: Gridded Population of the World, Version 4 (GPWv4): Population Density, http://beta.sedac.ciesin.columbia.edu/data/set/gpw-v4-population-density, 2016.

US Army Corps of Engineers: National Levee Database, https://levees.sec.usace.army.mil/#/.

Vafeidis, A. T., Nicholls, R. J., McFadden, L., Tol, R. S. J., Hinkel, J., Spencer, T., Grashoff, P. S., Boot, G., and Klein, R. J. T.: A New Global Coastal Database for Impact and Vulnerability Analysis to Sea-Level Rise, Journal of Coastal Research, 24, 917–924, https://www.jstor.org/stable/40065185, 2008.

von Krogh, G. and von Hippel, E.: The Promise of Research on Open Source Software, Management Science, 52, 975–983, https://doi.org/10.1287/mnsc.1060.0560, 2006.

Wilkinson, M. D., Dumontier, M., Aalbersberg, I. J., Appleton, G., Axton, M., Baak, A., Blomberg, N., Boiten, J.-W., da Silva Santos, L. B., Bourne, P. E., Bouwman, J., Brookes, A. J., Clark, T., Crosas, M., Dillo, I., Dumon, O., Edmunds, S., Evelo, C. T., Finkers, R., Gonzalez-Beltran, A., Gray, A. J. G., Groth, P., Goble, C., Grethe, J. S., Heringa, J., 't Hoen, P. A. C., Hooft, R., Kuhn, T., Kok, R., Kok, J., Lusher, S. J., Martone, M. E., Mons, A., Packer, A. L., Persson, B., Rocca-Serra, P., Roos, M., van Schaik, R., Sansone, S.-A., Schultes, E., Sengstag, T., Slater, T., Strawn, G., Swertz, M. A., Thompson, M., van der Lei, J., van Mulligen, E., Velterop, J., Waagmeester, A., Wittenburg, P., Wolstencroft, K., Zhao, J., and Mons, B.: The FAIR Guiding Principles for scientific data management and stewardship, Scientific Data, 3, 160 018, https://doi.org/10.1038/sdata.2016.18, 2016.

World Bank: International Comparison Program 2017, Database, https://www.worldbank.org/en/programs/icp#1, 2020.

https://doi.org/10.5194/egusphere-2022-198
Preprint. Discussion started: 6 May 2022

Yohe, G. and Tol, R. S.: Indicators for social and economic coping capacity - Moving toward a working definition of adaptive capacity, Global Environmental Change, 12, 25–40, https://doi.org/10.1016/S0959-3780(01)00026-7, 2002.

Yohe, G., Neumann, J., and Ameden, H.: Assessing the economic cost of greenhouse-induced sea level rise: methods and application in support of a national survey, Journal of Environmental Economics and Management, 29, S78–S97, 1995.

Zingerle, P., Pail, R., Gruber, T., and Oikonomidou, X.: The combined global gravity field model XGM2019e, Journal of Geodesy, 94, 1–12, https://doi.org/10.1007/s00190-020-01398-0, 2020.